

Master Thesis

## **Design and Simulation of an Electrostatically-Driven MEMS Micro- Mixer**



A master thesis submitted to the faculty of University of Bridgeport In partial fulfillment of the requirements for the degree of

**MASTER OF SCIENCE**

In the Department of Biomedical Engineering

By

Fei Mi

(Student ID: 862192)

B.S.(Clinic Medicine) Central South University, Changsha, China,  
August, 2003

July/2008 Thesis Advisor: Dr. Xingguo Xiong, University of Bridgeport,  
Bridgeport, CT 06604

## **ACKNOWLEDGMENT**

Nearly three-year graduate study in the major of BME, in UB has given me a good reorganization of Biomedical Engineering. Especially, in some applications of biomedical equipment which I have learnt in the course of MEMS is wonderful.

Firstly, I want to show my best gratitude to the Professor Patra, which is the Director of BME department. Before I have taken some courses from him, like Biomedical Materials, Fabrication of Nano-Materials and so on. He gave me a broad comprehension of the field of Biomedical Engineering so that I can develop the interests of the application of biomedical equipments which I take as the topic of my thesis.

Secondly, I want to say thank you to Dr. Xingguo Xiong, my co-advisor and good tutor, who gave me a well guide about how to do the thesis, including reading papers, making a decision of thesis idea, writing the abstract of thesis, and creating a basic frame of the thesis. Besides, he helped me solve the problems in some projects which I met in the process of doing my thesis.

Also, thanks for the coming the Professor Junling Hu and her good suggestions of how to prepare for the defense of the thesis.

Finally, I have to share the happy of the accomplishments of my thesis with my dear friends , who helped me a lot in the process of doing my thesis and support me since I did my thesis. In addition, I want to say thank you to my dear parents who have supported me all the time since I have started the study in this university.

## **ABSTRACT**

Bio MEMS ( Biology Micro-electro-mechanical Systems) focus on some micro-fabricated devices including electrical and mechanical parts to study the biological system such as new polymer-based drug delivery systems for anti-cancer agents, specialized tools for minimally invasive surgery, novel cell sorting systems for high-throughput data collection, and precision measurement techniques enabled by micro-fabricated devices. Especially some micro-liquid handling devices like micro-pumps, active and passive micro-mixers that can make two or more micro-fluids mixing completely, with the chaotic advection.

This kind of rapid mixing is very important in the biochemistry analysis, drug delivery and sequencing or synthesis of nucleic acids. Besides, some biological processes like cell activation, enzyme reactions and protein folding also require mixing of reactants for initiation, electrophoresis activation. Turbulence and inter-diffusion of them play crucial role in the process of mixing of different fluids.

In this report, it will introduce a new kind of electromechanical active micro-mixer, which includes two inlets and one outlet under the electrostatic driven voltage. Two different fluids will enter the micro-mixer and shows different colors separately blue and red. Choosing the ANSYS for the simulation of the fluids running in the micro-mixers, we can see nearly 100% fluids that have been mixed. ANSYS is used to show the effectiveness of the micro-mixer.

# TABLE OF CONTENTS

	PAGE
ACKNOWLEDGMENT.....	2
ABSTRACT.....	1
Chapter 1 Introduction.....	7
1.1 MEMS Technology.....	7
1.2 Aim for designing the micro-mixer: .....	7
1.3. What is micro-mixer? .....	7
1.4 Use of micro-mixers: .....	8
1.5 Background Information.....	8
1.5.1 History of Micro-mixers: .....	8
1.5.2 Development of active micro-mixers:.....	9
1.5.3 Application of micro-mixers:.....	10
1.5.4 Market and Future of Micro-Mixer:.....	10
1.6 Classifications of micro-mixer.....	10
1.6.1 Passive Micro-mixer: .....	10
1.6.2. Injection micro-mixer: .....	12
1.6.3 Chaotic advection micro-mixer:.....	13
1.6.4 Droplet micro-mixer: .....	13
1.7 Active micro-mixer:.....	14
1.7.1 Pressure disturbance micro-mixer:.....	14
1.7.2 Electro hydrodynamic disturbance: .....	14
1.7.3 Electrophoretic micro-mixer:.....	16
1.7.4 Electro kinetic micro-mixer: .....	16

1.7.5 Magneto Hydrodynamic Micro-mixer: .....	16
1.7.6 Acoustic micro-mixer: .....	17
1.7.7 Thermal disturbance micro-mixer:.....	17
1.7.8 Design with the piezoceramic buzzer (Figure 3); .....	17
1.8 Passive and active mixers .....	18
1.8.1 Comparison between active micro-mixers and passive micro-mixers:.....	18
1.8.2 Different designs of active and passive micro-mixers: .....	18
1.8.3 Different applications of active and passive micro-mixers:.....	19
1.9 Materials and fabrication process .....	19
1.9.1 The materials for fabricating the Micro-mixers:.....	19
1.9.2 Characteristics of some main materials .....	19
1.9.3 The fabrication process of micro-mixers .....	20
1.9.4. Two kinds of fabrication techniques:.....	20
1.9.5. Photolithography Process:.....	21
1.9.6. Etching Techniques.....	21
1.9,7 Other Fabrication Techniques:.....	24
1.9.8 Disadvantages and advantages of the Polymer materials .....	28
1.9.9. Two dimensional numerical simulation of chaotic flow:.....	28
Chapter 2 Transport Phenomenon In Microfluidic Mixer .....	30
2.1 Transport phenomenon of microfluidics in the micro-mixers .....	30
2.1.1 Fluid flow governing equations: .....	30
2.1.2 Electrophoresis in the transport of the microfluids:.....	30
2.1.3 Heat Transfer: .....	30
Chapter 3 Passive Micro-mixer Design and Simulation .....	31
3.1 Introduction of Passive Micro-mixers and Active Micro-mixers .....	31
3.2 Results and Discussions .....	33

Chapter 4 Design and Analysis of an Electrostatic Active Microfluidic Mixer .....	37
4.1. Introduction of new micro-mixer with electromechanical power.....	37
4.1.1 .Electromechanical design .....	37
4.1.2 Ansys simulation of electrostatic resonant plate.....	40
4.1.3 Matlab for driving voltage versus the normalized deflection for different plate thickness and resonant frequency versus the length of the plate .....	43
Chapter 5 Conclusions and Future Work.....	51
References:.....	52

## TABLE OF FIGURES

Figure 1.3 (Model 1) A Mobius band micro-mixer; (Model 2). of A straight channel these are two classic different types micro-mixers( <a href="http://www.google.com/images">http://www.google.com/images</a> ).....	8
Figure 1.5.2 3-dimension active micro-mixer[3].....	9
Figure 1.6.1(A) This is the parallel lamination micro-mixer: a). Basic T-mixer, b). Y-mixer, c). The concept of parallel lamination, d). The concept of hydraulic focusing. [6] .....	11
Figure 1.6.1(B) Serial lamination mixer: a). Join-split-join, b). Split-join, c). Split-split-join, d). Multiple intersecting micro channels. [9] .....	12
Figure 1.6.3 Planar design for mixing with chaotic advection at high Reynolds numbers: (a) obstacles on wall[12], (b) obstacles in the channels[13][14], (c) a zig-zag-shaped channel[15]. 13	
Figure 1.7.2 Model of electro-hydrodynamic disturbance micro-fluidic mixer [23].....	15
Figure 1.7.8 The micro-mixer with piezoceramic buzzer [20] .....	18
Figure 1.9.3 The fabrication procedure of the micro-mixer [23].....	20
Figure 1.9.6 (A): Illustration of how deep reactive ion etching works. [26] .....	22
Figure1.9.6 (B): SEM of a MEMS device fabricated using two sided DRIE etching technology on an SOI wafer. [26] .....	23
Figure 1.9.6(C): SEM of the cross section of a silicon wafer demonstrating high-aspect ratio and deep trenches that can be fabricated using DRIE technology [26].....	23
Figure 1.9.6(D): SEM of high aspect ratio structures etched into a glass substrate fabricated by MNX. [26] .....	24
Figure 1.9.7(A): An illustration of the steps involved in the LIGA process to fabricate high aspect ratio MEMS devices. ....	25
Figure 1.9.7(B): A tall, high aspect ratio gear made using LIGA technology.....	25
Figure 1.9.7 (C): Illustration of the hot embossing process to create micro devices. (Courtesy of the MNX at CNRI). [27].....	26
Figure 1.9.7(D): Photograph of a hot embossing platform during use.(Courtesy of the MNX at CNRI). [27].....	27

Figure 1.9.7(E): SEM of a variety of small test structures made in a plastic substrate using hot embossing technology at the MNX. The height of the plastic microstructures is nearly 300  $\mu\text{m}$  and the smallest features have a diameter of about 25  $\mu\text{m}$ . (Courtesy of the MNX at CNRI). [27] ... 27

Figure 1.9.9	CFD simulation of Chaotic flow in a VLM at $\text{Re}=0.64$ .....	28
Fig.3. 2A	Meshed ANSYS model of mixer.....	33
Fig. 3.2 B	Contour plot of density distribution.....	34
Figure 3.2 C	Ansys Fluid Velocity Vector Plot.....	34
Figure 3.2 D	Local View of Induced Turbulence.....	35
Figure 3.2 E	Density Distribution Near Inlet.....	35
Figure 3.2 F	Density Distribution at Outlet .....	36
Fig. 3.2G	Density plot ( $\rho_2=35\text{g/cm}^3$ ).....	36
Figure 4.1.1(A)	2-dimension electrostatically activated resonant micro-mixer .....	37
Figure 4.1.1(B)	3 views from different angles of the 3-dimension active micro-mixer.....	39
Figure 4.1.2 (1)	Figure a,b,c,d are four stages which in the process of the fluctuation of the electrostatic resonant plate.....	41
Figure 4.1.2 (2)	This figure just shows three different frequencies.....	42
Figure 4.1.3 A	Relationship between voltage and displacement of resonant plate ( $h=1\mu\text{m}$ , Matlab) .....	44
Figure B	Relationship between Voltage and Displacement of Resonant Plate ( $h=1.5\mu\text{m}$ , Matlab) .....	45
Figure C.	Relationship between Voltage and Displacement of Resonant Plate ( $h=2\mu\text{m}$ , Matlab).....	46
Figure D	Comparison in three different thickness Matlab( $h=1\mu\text{m}, 1.5\mu\text{m}, 2\mu\text{m}$ ) .....	47
Figure 4.1.3	Ansys for the plate which applied to a electrode plate (a. b. c. are three ansys simulation results and d is the results of the displacement of the resonant plate which is under the electrostatic force).....	49



# Chapter 1 Introduction

## 1.1 MEMS Technology

Nowadays with the development of MEMS technology, there are some equipment which we use on the biology analysis, experiment tests, chemistry industry, especially some equipments which we use on the biomedical technologies such as micro-pump, micro-filter, micro-valve, micro-mixer, micro-actuator, micro-sensor, micro-reactor, micro-channel, just trying to narrow down those equipments to micro-scale, mainly integrating these micro-scale facilities into a lab-on-a-chip for the aims of bio-chemical disposal, diseases diagnose, analytical examination, new drug development and monitoring environment and so on [1].

## 1.2 Aim for designing the micro-mixer:

The micro-technology can make the mixing of micro-fluidics be more well-distributed and faster than any other normal mixing equipment, especially in the areas of chemical synthesis, emulsion liquid preparation. According to the Frick law, increasing the contact area between two different fluids can accelerate the mixing. So we just generate the turbulent flow that we can the effects of mixing. Here we just investigate the mixing of fluids in micro-scale; the Reynolds number is far less than the Reynolds number when turbulent occurs. The final aim is how to make two or more different fluids mix completely and enhance the efficiency.

## 1.3. What is micro-mixer?

Micro-mixers can be separated into two different kinds including: active and passive. In active micro-mixers, some controlled movable parts or external disturbances will be integrated into the system. There are some classic external powers such as: pressure gradient, temperature gradient, electric field force, magnetic force, thermal convection and acoustic wave so on. The advantage of using the active micro-mixers is that some movable elements or additional disturbances can be controlled to obtain effective mixing.

Another kind of micro-mixers is passive micro-mixer. In passive micro-mixers, it just utilizes the change of geometrical shape of channels or characteristics of micro-fluidics to advance the mixing results. The principle of this kind of micro-mixers is that it depends on the molecular diffusion, chaotic advection or turbulence effect without using external disturbances. The passive micro-mixers are cheaper than the active micro-mixers and require suitable for high efficiency.

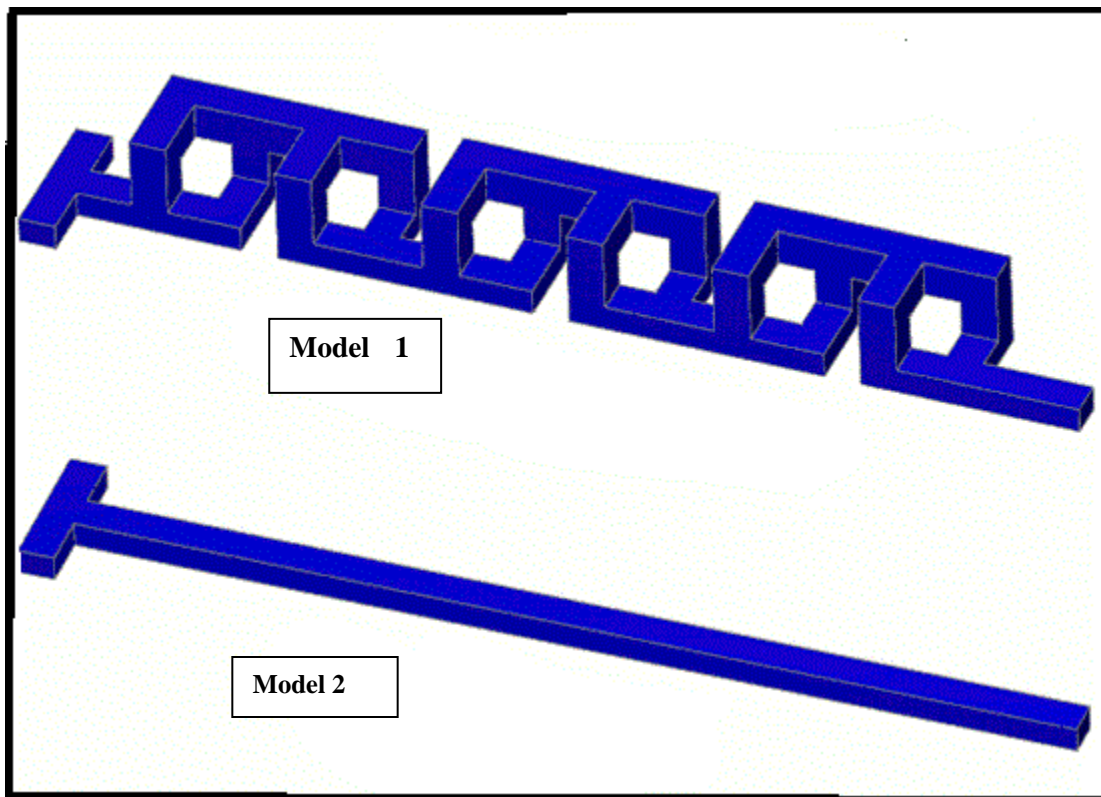


Figure 1.3 (Model 1) A Möbius band micro-mixer; (Model 2). of A straight channel these are two classic different types micro-mixers(<http://www.google.com/images>).

#### 1.4 Use of micro-mixers:

DNA sequencing, sample preparation and analysis, cell separation and detection will use the micro-mixers systems. Besides, in some biological processes such as cell activation, enzyme reactions, protein folding, drug delivery and sequencing or synthesis of nucleic acids.

#### 1.5 Background Information

##### 1.5.1 History of Micro-mixers:

In 2001, S. Bthm and others invented a fast vortex micro-mixer which can be used for high-speed chemical reaction, in this design the micro-mixer can reduce the diffusion distances by using vortex (cyclonic fluid field would exist in this vortex chamber and it can reduce the distance between

In 2002, Seck Hoe Wong and some other scientists reported that a T-micro-mixer. This kind of micro-mixer just needs a few milliseconds for mixing. Although it is very difficult to produce the turbulence in the micro-channels, it can mix the micro-fluids quickly through the secondary flow, swirling flow and vortex.

In 2003, Bessoth and some other people designed a crossing dividing- recombining micro-mixer. The basic working principle is: this kind of micro-mixer just divided micro-fluids into many thin layers of fluid flows to shorten the diffusion distance between fluids flow and mixing time. This kind of micro-mixers has some characteristics including: short reaction time, low consumption of the reagents and samples, easy to be miniaturization and automation.

### 1.5.2 Development of active micro-mixers:

In 2001, Zhen Yang reported an ultrasonic micro-mixer that can be used for continuous fluids. Input, output and mixing chamber can form on the top of glass and all the circuit is wrapped with the anodic bonding between the silicon wafer and glass pieces. In the meantime, Bau created another magnetic power driven micro-mixer, whose channels contained lots of electrolyte solution.

Then Frederic Bottausci developed a 3-dimension active micro-mixer. The fluid in the main channel would be affected by 3-pairs of disturbed jets which were controlled by pump. When change the frequency and amplitude of the branch channel of the micro-mixer, the flow pattern would change.[Figure 2.1.1]

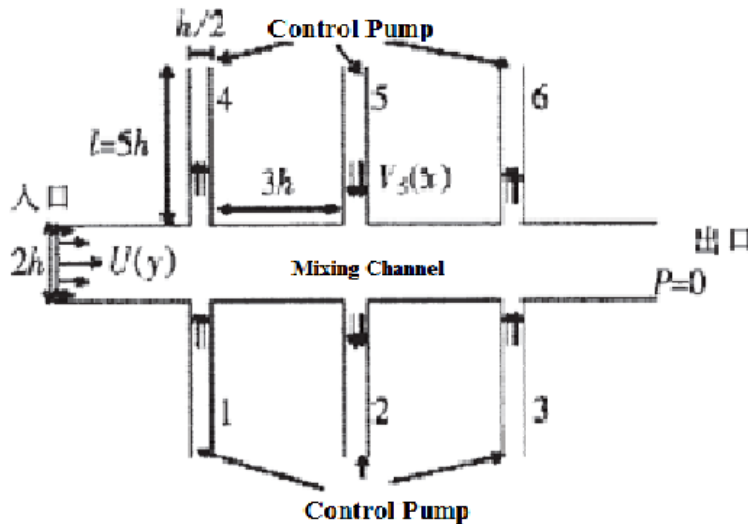


Figure 1.5.2 3-dimension active micro-mixer[3]

Peter Huang and some other people reported an electroosmotic micro-mixer, this kind of micro-mixer could disturb two fluids fast with the electrostatic power. The mixing effects are related with electric field, frequency and fluid flow, and it can be measured by the intensity distribution of the downstream of mixing area.

### **1.5.3 Application of micro-mixers:**

The micro-mixing technology can be applied to many areas, like fast mixing, chemical synthesis, emulsion preparation, high throughput and biochemistry. Besides, the MEMS micro-mixers can be used for lab-on-a-chip, digital microfluidics, micro-drug delivery system and some other BIO-MEMS applications.

Take the application of lab-on-a-chip for example, in the past decade, there is a broad utilization in biology, medicine and chemistry, that includes sample preparation, mixing, reaction, injection, separation analysis and detection in detail[2][3].

The application fields of micro-mixers can cover modern and specialized issues, like sample preparation for chemical analysis and traditional, widespread usable mixing tasks including reaction, gas absorption, emulsification, foaming, and blending.[4] Micro-mixer elements, micro-mixers, and micro-structured mixers typically have flows in the sub-ml/h, ml/h-l/h and 10-10,000 l/h ranges, covering the whole flow range up to the conventional static mixers and being applied to chemical production as well.

### **1.5.4 Market and Future of Micro-Mixer:**

Generally speaking, passive micro-mixers mainly increase diffusion and convection of molecules to change the geometric shape, and then expand the micro-fluids contact surface and mixing efficiency. So the shapes of passive micro-mixers usually are very complicated and it is a little difficult to fabricate.

## **1.6 Classifications of micro-mixer**

### **1.6.1 Passive Micro-mixer:**

#### **A). Parallel lamination micro-mixer:**

In parallel lamination micro-mixers, the parallel lamination splits the inlet streams into  $n$  sub-streams and then joins them into one stream as laminar. For the basic T-mixer, the inlet streams of T-mixer can be twisted and laminated as two thin liquid to reduce the mixer channel. The molecular diffusion and chaotic advection are very important for the T-mixer. When the mixing channel is very long, the T-mixer mainly depends on molecular diffusion; when the mixing channel is short, the mixer mainly depends on the chaotic advection. Another shape of this kind of micro-mixer is Y-mixer, which needs fast vortices to mix multiple inlet streams quickly and completely. This mixer (T-mixer) utilizes Reynolds numbers up to 500, where flow velocity can be as high as  $4.60 \text{ m s}^{-1}$  at a driven pressure of up to 7 bar [6]. Under extremely high Reynolds numbers ( $Re = 245, 45 \text{ m s}^{-1}$ ) a fluid flow can also generate high shear to drive very fast circulation in a diamond-shaped cavity close to a straight micro channel[7]. Both of these two kinds of micro-mixer need to be improved by reducing the mixing paths. Through narrowing the mixing channel and hydrodynamic focusing, the mixing channel can be decreased. Take the

basic hydrodynamic focusing micro-mixer for example, there are three inlets which induce sample flow and sheath flows. The sample flow is in the middle and the other two flows runs like sheath flows. Figure 1.6.1 shows the T-mixer, Y- mixer, the three flows after improvement for reducing the mixing paths.

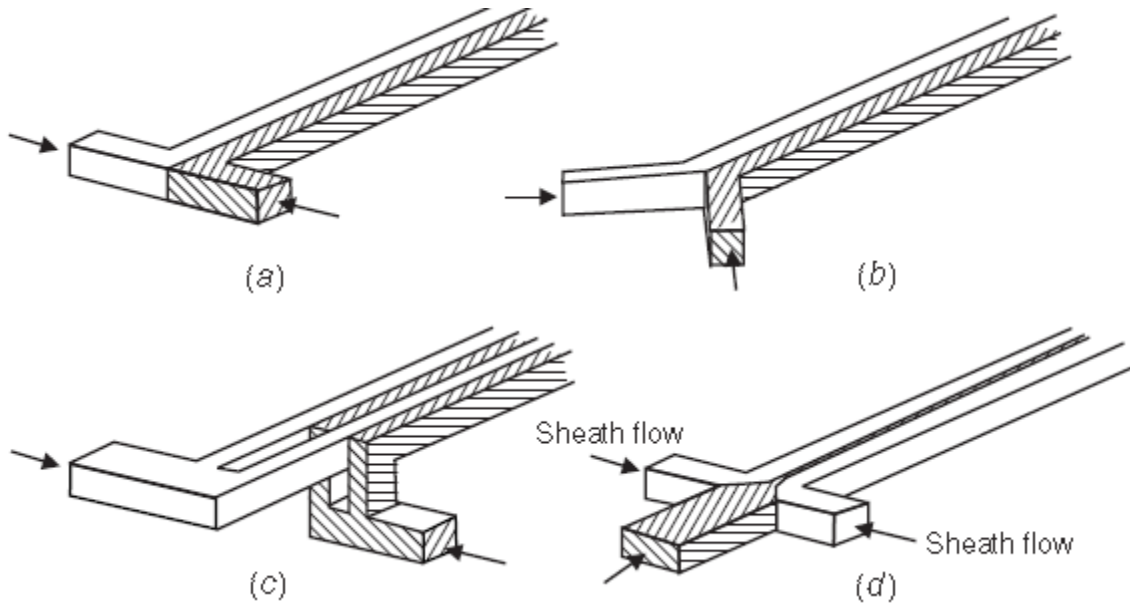


Figure 1.6.1(A) This is the parallel lamination micro-mixer: a). Basic T-mixer, b). Y-mixer, c). The concept of parallel lamination, d). The concept of hydraulic focusing. [6]

**B). Serial Lamination Micro-mixer:**

As the parallel lamination micro-mixer, serial lamination micro-mixers also experience splitting and joining the streams [8]. Here the inlet streams firstly joined horizontally and then go along vertical channels. Figure 1.6.1 (B) shows the serial lamination micro-mixers.

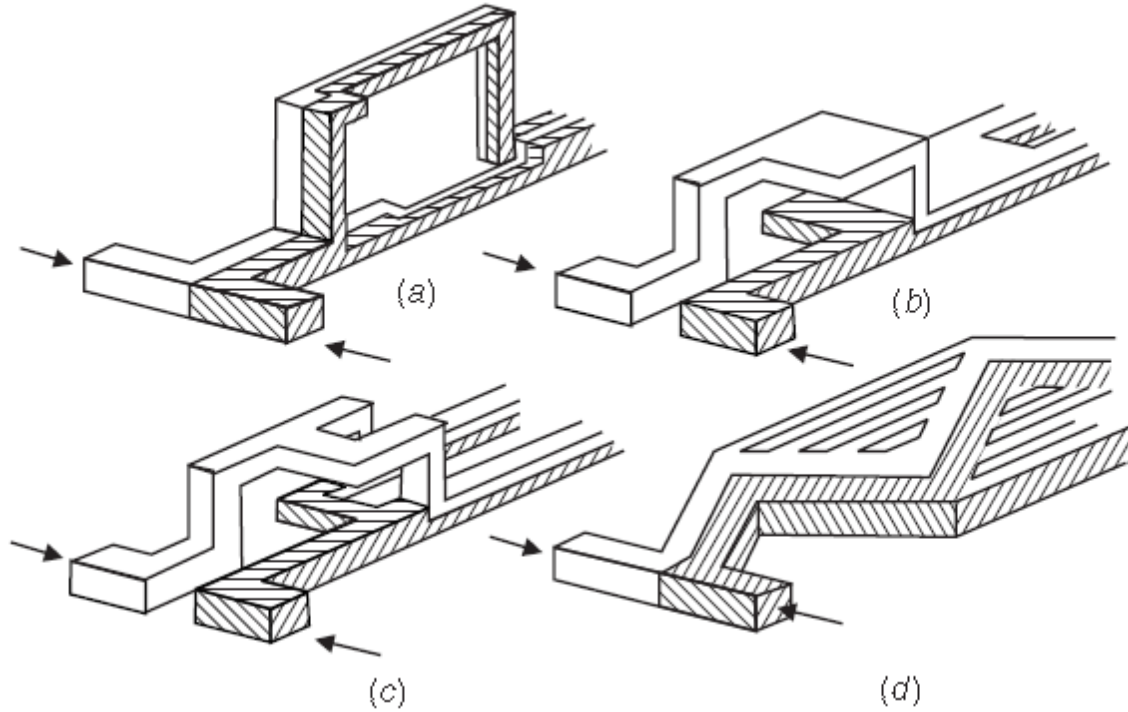


Figure 1.6.1(B) Serial lamination mixer: a). Join-split-join, b). Split-join, c). Split-split-join, d). Multiple intersecting micro channels. [9]

### 1.6.2. Injection micro-mixer:

This kind of micro-mixer is similar to the parallel lamination mixer, but not splitting both inlet flows and only splitting the solute flow into many streams and injecting then into the solvent flow. There are lots of nozzles on top of one stream which create a number of micro plumes of the solute. These plumes just increase the contact surface and decrease the mixing path. The nozzle array is installed in a mixing chamber which is fabricated from silicon using DRIE. There is an equation [31] which describes the dimensionless concentration:

$$c^*(r^*, \theta) = \frac{K_0(Per^*/4)/Pe}{K_1(Pe/4) - K_0(Pe/4)\cos\theta \times \left\{ \exp[Pe(r^* - 1)/4] \right\}^{\cos\theta}}$$

(1.6.2)

- $\theta$  is the angle (rad);
- $C^*$  is the dimensionless concentration ( $kgm^{-3}$ );
- $r^*$  is the dimensionless radius (m);

- $Pe$  is the Peclet number;
- $Re$  is the Reynolds number;
- $Kn$  is the modified Bessel function of the second kind  $n$ -order;

In the process of mixing, one area has been filled with one liquid, and other liquid is injected into the area through some micro-nozzles and many micro-plumes can be created to increase the contact surface between two liquids [9][10].

### 1.6.3 Chaotic advection micro-mixer:

When the Reynolds number is very low, it is very important to use the principle of chaotic advection that can be created by some special geometries of the mixing channel. Here the micro-mixers are like the macro-scale mixers, and the chaotic advection is dependent on the rips and grooves which are on the channel wall. The grooves are ablated on the bottom wall using a laser whose structure allows an electro kinetic flow to mix at a relatively slow velocity of  $300 \mu\text{m/s}$ . These micromixers can be fabricated by excimer laser ablation on a polycarbonate sheet covered with PETG.

[11]When the Reynolds number is very high, it is necessary to insert obstacles structures in the mixing channel, and use the zig-zag microchannels to produce recirculation around the turns to generate chaotic advection. The total mixing length was about 20mm, and the chaotic advection can be generated at  $Re=25-70$  and the mixing process is faster at a higher Reynolds number.

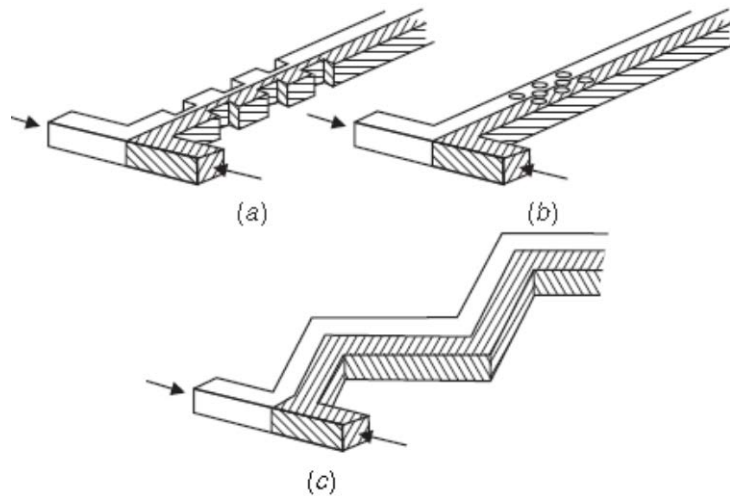


Figure 1.6.3 Planar design for mixing with chaotic advection at high Reynolds numbers: (a) obstacles on wall[12], (b) obstacles in the channels[13][14], (c) a zig-zag-shaped channel[15]

### 1.6.4 Droplet micro-mixer:

We just create droplets by using the pressure or capillary effects such as thermo capillary and electro wetting, or different surface forces in a small channel with multiple immiscible phases

such as oil/water or water/gas. Through merging and splitting repeatedly we can get the droplets, which can be transported by using the electro wetting. The other droplet micro mixer design used flow instability between two immiscible liquids. To form the aqueous samples we may use a carrier liquid like oil. The shear force between carrier liquid and sample may accelerate the mixing process in droplet.

The earliest droplet micro-mixer was fabricated in PDMS and covered with a PMMA sheet.

Droplet can be driven by electro wetting and the flow instability between two immiscible liquids.

## **1.7 Active micro-mixer:**

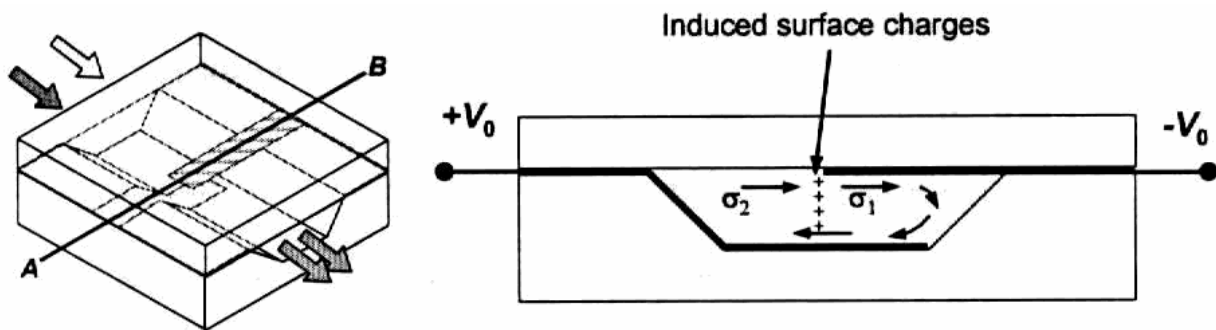
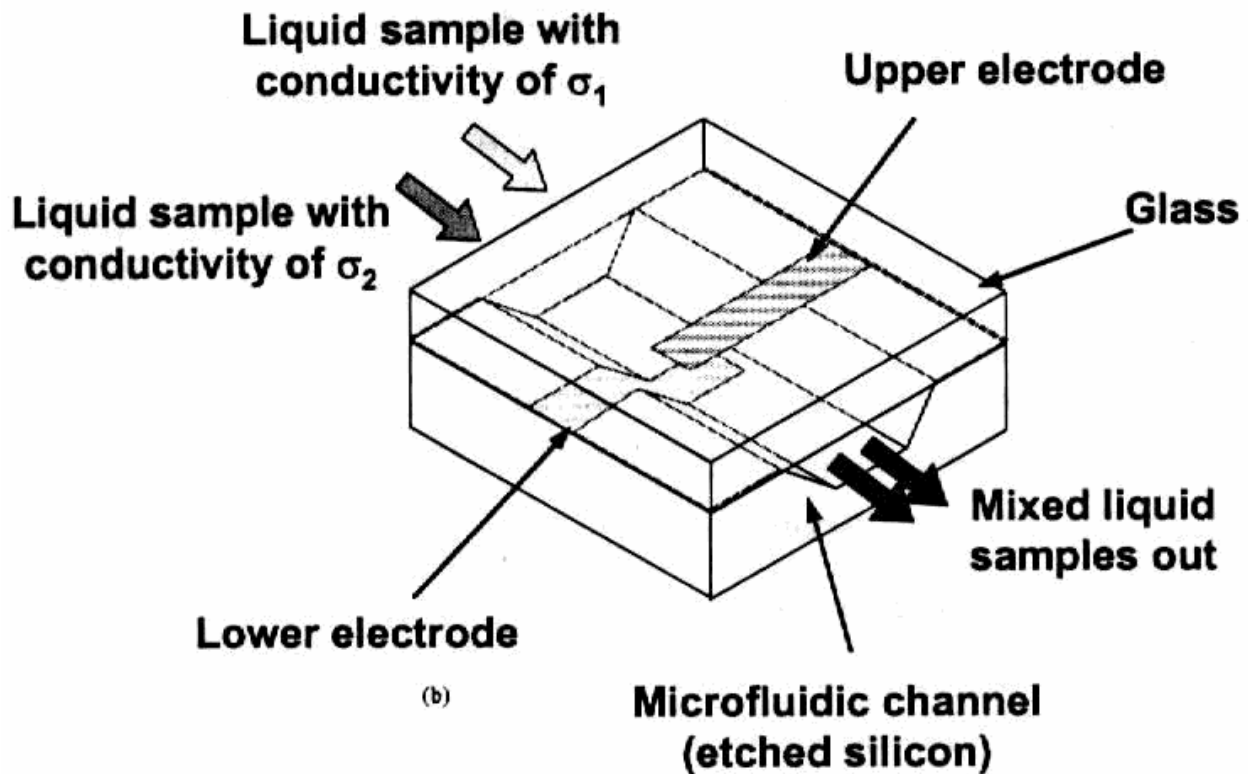
### **1.7.1 Pressure disturbance micro-mixer:**

The micro-mixer-- pressure micro-mixer, can be integrated in a microfluidic system which is fabricated in silicon using DRIE. There is a special device--planar micro pump which can drives and stops the flow in the mixing channel to divide the mixed liquids into serial segments and make the mixing process independent of convection.

For producing the pressure disturbance, there are two ways including utilizing an external micro pump and pulsing velocity. When using the pulsing velocity, the simulation of micro-mixer is created with the pulsed side flow at a small Reynolds number of 0.3 and a computer controlled source-sink system.

### **1.7.2 Electro hydrodynamic disturbance:**





- Surface charges are induced at the interface
- External electric fields make the induced charges move
- Moving charges produce the shear force
- Liquids are moving along with the induced charges and being mixed

Figure 1.7.2 Model of electro-hydrodynamic disturbance micro-fluidic mixer [23]

Figure 1.7.2 is a simple geometry micro-mixer which utilizes the electro-hydrodynamic force to mix those fluids that have different electric properties and are subjected to an electric field. In

this model, the electrodes can produce an electric field which is perpendicular to the direction of the fluid flowing, and then a transversal secondary flow emerges. [16] A series of titanium wires is placed in the direction perpendicular to the mixing channel. By changing the voltage and frequency on the electrodes good mixing was achieved after less than 0.1 s at a low Reynolds number of 0.02.

### **1.7.3 Electrophoretic micro-mixer:**

In electrophoretic micro-mixer, there is a particle suspending in a medium of different dielectric characteristics becomes electrically polarized, and then the polarized particle can move either to the area of high or low electrical field intensity in according to the difference between the polarization of particle and medium. Before that, the particles in the DEP micro mixers are forced by the DEP force to move to and from an electrode. [17]The electrophoretic force will decrease with distance from the electrode edge that means once the particle is “trapped” by positive DEP, strong fluid velocity have to generate sufficient drag to overcome the electrophoretic force. On the contrary, a negative DEP would repel particles attracted to electrode edges when the particles are located in a low velocity area. In the meantime, fluid velocity must be in a low level that the DEP force can conquer the fluid drag on those particles, (fluid velocity: 100 $\mu$ m/second; voltage:  $\pm$ volts; gap: 10/20 $\mu$ m). It is a very interesting phenomenon that nowadays the chaotic advection was generated by embedded particles with a combination of electrical actuation and local geometry channel variation. Besides, a new DEP micro-mixer is using the parallel microelectrodes to manipulate the polymer particles and create vortex which can stir fluid to achieve mixing.

### **1.7.4 Electro kinetic micro-mixer:**

Electrokinetic mixing is effected using a single voltage source with the channels dimensioned to perform the desired voltage division [18]. Besides, the number of fluid reservoirs decreases because of the terminating multiple buffer. In this kind of micro-mixer, it uses electrokinetic flow to transport liquid. It does not need the external pumps to create chaotic advection pulsatile flow. Besides, the micro-mixer can introduce an AC voltage to create the oscillating electro-osmotic flow in a mixing chamber. Through switching on or off the voltage applied to the flow generates fluid segments in the mixing channel.

### **1.7.5 Magneto Hydrodynamic Micro-mixer:**

In this kind of micro-mixers, an external magnetic field applied dc voltages on the electrodes can generate Lorentz forces, which can roll and fold the liquids in a mixing chamber and make the fluids to mix completely. For example, there is a new magneto hydrodynamic micro-mixer named a minute magneto hydrodynamic micro-mixer, including an array of electrodes depositing on a conduit's walls, which are filled with an electrolyte solution, and then choosing alternating voltage across pairs of electrodes to create various directions of currents in the solution. Coupling created between the magnetic and electric fields induces body forces in the fluid [19]. Besides, complex flow fields can be created through the patterned electrodes generated in various ways.

### **1.7.6 Acoustic micro-mixer:**

In this kind of micro-mixer, acoustic actuators will be applied to the process of stirring fluids. Through changing the frequency and the voltage of the input signal, the vibration can be controlled. The acoustic micro-mixer will use loosely focused acoustic waves to generate stirring movements, drive the actuator and the wave is driven by a piezoelectric metallic oxide thin film.

### **1.7.7 Thermal disturbance micro-mixer:**

In this kind of micro-mixer, thermal energy is introduced to enhance mixing. There are mainly including two kinds of thermal disturbance micro-mixers, one is to create a linear temperature gradient through the channels and another one is to produce a thermal bubble .In the process of mixing micro-fluids, thermal diffusion and convection can be used to control the heat transfer.

### **1.7.8 Design with the piezoceramic buzzer (Figure 3);**

A>.This kind of piezoceramic buzzer is under the agitation of piezoceramic buzzer, and SU-8 can be used to fabricate the microstructure and piezoceramic buzzer to obtain the agitation. Here the converse piezoelectric effect could be utilized to generate the required piezoelectric induced strain with the electric field [20].

B>. Fabrication of micro-mixers with piezoceramic buzzer:

1). A thin film will be stuck on the top of SU-8 structure to seal the mixing chamber and the microchannels. UV adhesive FP-4272 will be used to form the diaphragm and PDMS be used as the substrate. Casting the PDMS in a container and then bake it to form a film. The PDMS substrate would be spun to create a uniform layer of UV adhesive on the surface of PDMS with UV adhesive FP-4272 so that the PDMS substrate could be adhered to SU-8 micro-mixer structure.

2). Then peeling PDMS off, cutting off the inlet and outlet regions and gumming 3 tubes.Finally, the piezoceramic buzzer is bonded to the top cover of mixing chamber. In the piezoceramic buzzer,the piezoceramic element is glued to a vibration plate and an alternating voltage output drives the piezoceramic element to expand or to shrink to cause the plate vibrating .Then the shape of diaphragm will be changed.

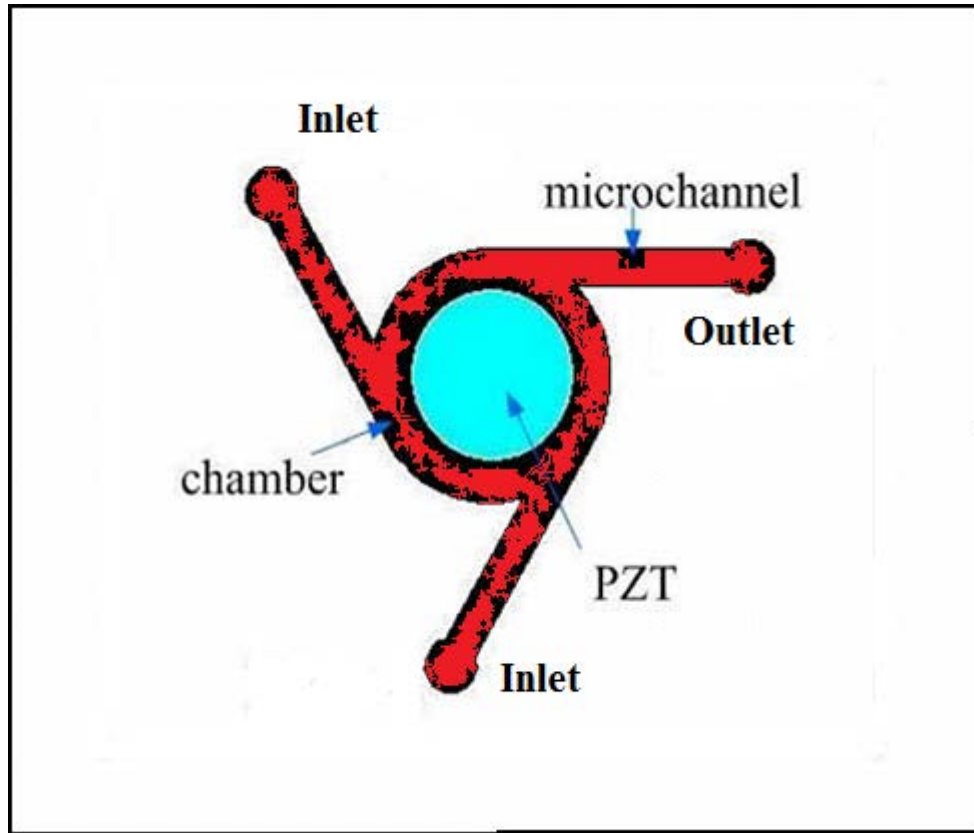


Figure 1.7.8 The micro-mixer with piezoceramic buzzer [20]

## 1.8 Passive and active mixers

### 1.8.1 Comparison between active micro-mixers and passive micro-mixers:

In passive micro-mixers, they can disturb the micro-fluids without external energy but only need the diffusion or chaotic advection. Whereas, the active micro-mixers need using external power including pressure, temperature, electrohydrodynamics, dielectrophoretics, electrophoretics, electrokinetics, magnetohydrodynamics and acoustics to work. After integration with these external fields, the structures of active micro-mixers are often complicated and the process of fabrication is complex. In contrast, passive structures are stable to operate and easily integrated in a system.

### 1.8.2 Different designs of active and passive micro-mixers:

In passive micro-mixers, they just need some simple geometry without external power to be added into the micro-mixers, like complicated 3-dimension structures. In active micro-mixers, some external input powers need to be integrated into the mixers, such as acoustic wave, heat, magnetic field and so on.

### **1.8.3 Different applications of active and passive micro-mixers:**

Micro mixers can be used in chemical, biological and medical analysis fields. For example, some basic T-mixers can be used for the measurement of analyte concentrations of a continuous flow. (The concentration of a target analyte is measured by the fluorescence intensity of the region where the analyte and a fluorescent indicator have interdiffused.)

Besides, the micro-mixer can be used for the study of rapid chemical reaction in solution with stopped-flow time resolved Fourier transform infrared spectroscopy. The principle is to achieve lamination of two liquid sheets of 10 $\mu$ m thickness and ~1mm width on top of each other and operate in stopped-mode [21]. Also micro-mixers can be used as sensors in environmental monitoring such as the detection of ammonia in aqueous solutions [22]. An electrokinetically driven T-mixer is used for performing enzyme assays and a T-mixer which is combined with the capillary electrophoresis separation can be used as a postcolumn reactor. The micro-mixers. In addition, micromixers were used to disperse immiscible liquids and form micro droplets. Furthermore, micro-mixers can work as a separator for particles based on their different diffusion coefficients or as a generator of concentration gradients.

## **1.9 Materials and fabrication process**

### **1.9.1 The materials for fabricating the Micro-mixers:**

Usually micro-mixers combine some original functional elements like micro-pump, micro-valve, micro-electrodes, micro-checking original elements, connector and so on. The materials have changed from the primary silicone to glass, SiO<sub>2</sub>, metal and organic polymers and so on, including epoxy resin, PMMA, PC, PDMS.

The main material which is used to fabricate the micro-mixers is PDMS, which has high bio-compatibility with the biology carrier, easy to be made and is transparent, non-toxic and suitable to the optic examination. Besides, silicon will be used to form the actuators which would be integrated into some active micro-mixers. Besides, glasses, ITO, gold and polyester are suitable substrate materials.

### **1.9.2 Characteristics of some main materials**

#### **1> Five kinds of main materials:**

Silicone and the silicon dioxide have good chemical laziness and heat stability, and these two kinds of materials can be used for fabricating micro-channels. Besides, silicon materials are fragile, costly, opaque, low electric insulativity and complicated chemical behaviors so that it cannot be applied widely in micro-channels. However, it can be used to fabricate micro-pump, micro-valve and some fluid driven and control elements.

Glass and quartz have good electricity penetration and optical property, surface wettability, surface absorption and surface reaction. Using the photolithography and etching can copy the micro-net onto the glass or quartz chip.

High polymers are easy to select, fabricating, and contains many kinds. With this kind of materials, we can produce a mass of disposable micro-net.

### 1.9.3 The fabrication process of micro-mixers

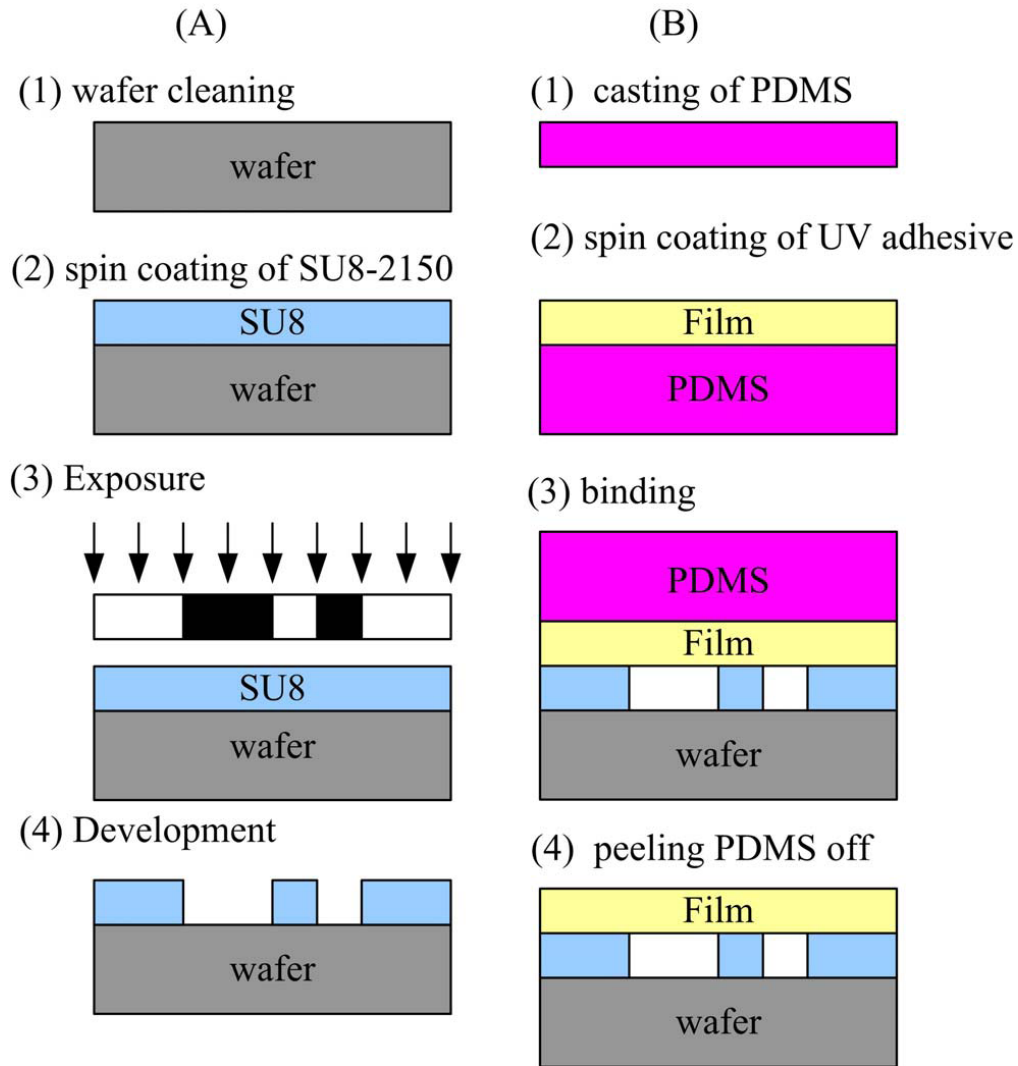


Figure 1.9.3 The fabrication procedure of the micro-mixer [23]

### 1.9.4. Two kinds of fabrication techniques:

Most early micro-mixers were made of silicon, the mixing channels were either wet etched with KOH or dry etched with ion etching.

#### 1> Dry etching fabrication

Generally speaking, there are 3 steps including laminating, patterning and curing the dry resist layer before the lamination of next layer. Brass shims, glass, ITO, gold, polyester and metal are the substrate material. Metal can be injected or evaporated onto the dry film resist to produce electrodes for special application. Specifically speaking, the dry film resist is first laminated at a

certain temperature, then using an appropriate mask, dry film resist is exposed to an around 100mv at 330 nm UV light. The height of the channel can be varied by using dry film of appropriate thickness. [23]

2> Wet etching fabrication: [24]

In general, in passive micro-mixers, the most important material which is used to fabricate micro-mixers is PDMS, that has high bio-compatibility, easy to make, nontoxic, transparent, and suitable for the optic test. There are 3 steps, firstly, put some SU8 thick film photo-resist on the wafer, then start the yellow light fabrication; secondly, keep the SU8 photo-resist on the pattern and mix PDMS and curing agent according to the ratio of 10:1; thirdly, pump the bulb in the PDMS and pour the mixture onto SU8 photo-resist for the baking. Finally, take off it under the wafer and put it into ICP for surface oxygen plasma processing, then we can get the micro-channels.

### **1.9.5. Photolithography Process:**

In the active micro-mixers, firstly, we need to deposit Al to the glass, then start the yellow light fabrication. Secondly, using Al etchant to get resistive heater and putting it into ICP for changing surface hydrophilic characteristics.

There are mainly including four steps: substrate pretreatment, coating photoresist, soft bake and exposure. Firstly, using the silicon wafer as the substrate and wafer surface which should be cleaned for being coated with the SU-8 by a spin coating; then soft baking, that is baking the photoresist onto a hot plate to remove the excess photoresist solvent. Next, using exposure process with a certain length (depends on the type of micro-mixers) of UV light to get some hole deep into the wafer and spinning new resist to cover the surface of the hole on the wafer; Finally, using some SU-8 developer to dissolve the photoresist on the surface of wafer and transfer the pattern to the back of the wafer for making the inlet and outlet with the same method. [25]

### **1.9.6. Etching Techniques**

#### **1). Deep Reactive Ion Etching of Silicon**

Deep reactive ion etching or DRIE is a relatively new fabrication technology that has been widely adopted by the MEMS community. This technology enables very high aspect ratio etches to be performed into silicon substrates. The sidewalls of the etched holes are nearly vertical and the depth of etching can be hundreds or even thousands of microns into the silicon substrate.

Figure 1.9.6 (A) illustrates how deep reactive ion etching is accomplished. The etching is dry plasma etching and uses high density plasma to alternately etch the silicon and deposit an etching resistant polymer layer on the sidewalls. The etching of the silicon is performed using an SF<sub>6</sub> chemistry whereas the deposition of the etching resistant polymer layer on the sidewalls uses C<sub>4</sub>F<sub>8</sub> chemistry. Mass flow controllers alternate back and forth between these two chemistries during the etching. The protective polymer layer is deposited on the sidewalls as well as on the bottom of the etch pit, but the anisotropy of the etching removes the polymer at the bottom of the etch pit faster than the polymer is removed from the sidewalls. The sidewalls are not perfectly smooth and if the sidewall is magnified under SEM inspection, a characteristic washboard or scalloping pattern is seen in the sidewalls. The etch rates on most commercial DRIE systems varies

from 1 to 4 microns per minute. DRIE systems are single wafer tools. Photoresist can be used as a masking layer for DRIE etching. The selectivity with photoresist and oxide is about 75 to 1 and 150 to 1, respectively. For a through wafer etch a relatively thick photoresist masking layer will be required. The aspect ratio of the etching can be as high as 30 to 1, but in practice tends to be 15 to 1. The process recipe depends on the amount of exposed silicon due to loading effects in the system, with larger exposed areas etching at a much faster rate compared to smaller exposed areas. Consequently, the etching must frequently be characterized for the exact mask feature and depth to obtain desirable results.

Figure 1.9.6 (B) is a SEM of a MEMS component fabricated using DRIE and wafer bonding. This device was made using an SOI wafer wherein a backside etch was performed through the handle wafer, stopping on the buried oxide layer, and a front side DRIE was performed on the SOI device layer. Then the buried oxide was removed to release the microstructure, allowing it to freely move.

Figure 1.9.6 (C) is a cross section SEM of a silicon microstructure fabricated using DRIE technology. As can be seen, the etching is very deep into the silicon substrate and the sidewalls are nearly vertical.

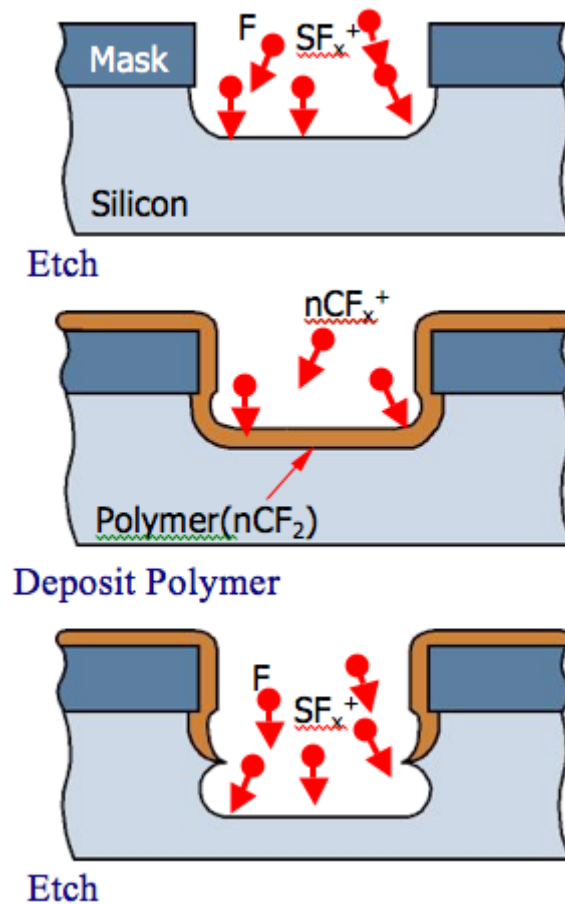


Figure 1.9.6 (A): Illustration of how deep reactive ion etching works. [26]



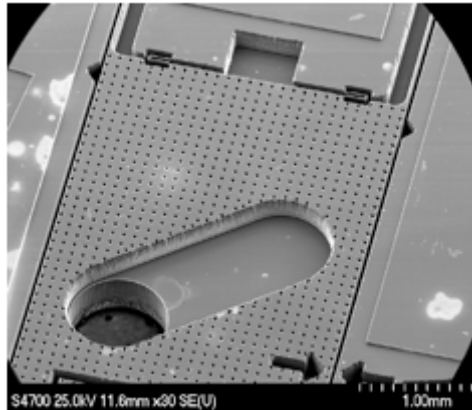


Figure 1.9.6 (B): SEM of a MEMS device fabricated using two sided DRIE etching technology on an SOI wafer. [26]

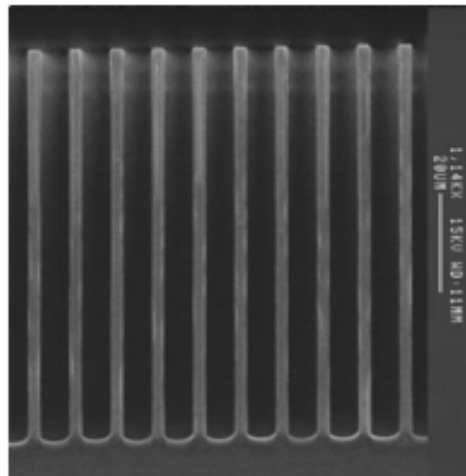


Figure 1.9.6(C): SEM of the cross section of a silicon wafer demonstrating high-aspect ratio and deep trenches that can be fabricated using DRIE technology [26]

## 2). Deep Reactive Ion Etching of Glass

Glass substrates can also be etched deep into the material with high aspect ratios and this technology has been gaining in popularity in MEMS fabrication. Figure 5.2.3 (D) shows a structure fabricated into glass using this technology. The typical etch rates for high aspect ratio glass etching range between 250 and 500 nm per minute. Depending on the depth of the photoresist [26]

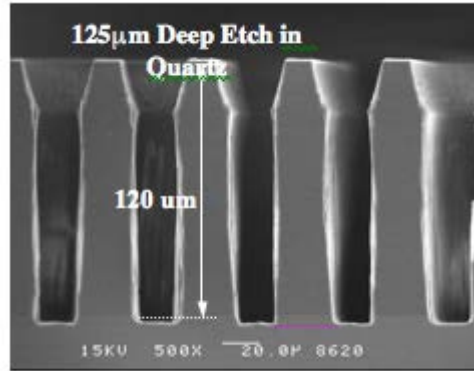


Figure 1.9.6(D): SEM of high aspect ratio structures etched into a glass substrate fabricated by MNX. [26]

## 1.9,7 Other Fabrication Techniques:

### 1). LIGA

Another popular high aspect ratio micromachining technology is called LIGA, which is a German acronym for “Lithography Galvanoformung Adformung.” This is primarily a non-silicon based technology and requires the use of synchrotron generated x-ray radiation. The basic process is outlined in Figure 1.9.7(A) and starts with the cast of an x-ray radiation sensitive PMMA onto a suitable substrate. A special x-ray mask is used for the selective exposure of the PMMA layer using x-rays. The PMMA is then developed and will be defined with extremely smooth and nearly perfectly vertical sidewalls. Also, the penetration depth of the x-ray radiation into the PMMA layer is quite deep and allows exposure through very thick PMMA layers, up to and exceeding 1 mm. After the development, the patterned PMMA acts as a polymer mold and is placed into an electroplating bath and Nickel is plated into the open areas of the PMMA. The PMMA is then removed, thereby leaving the metallic microstructure (Figure 1.9.7(B)).

Because LIGA requires a special mask and a synchrotron (X-ray) radiation source for the exposure, the cost of this process is relatively expensive. A variation of the process which reduces the cost of the micro machined parts made with this process is to reuse the fabricated metal part (step 5) as a tool insert to imprint the shape of the tool into a polymer layer (step 3), followed by electroplating of metal into the polymer mold (step 4) and removal of the polymer mold (step 5). Obviously this sequence of steps eliminates the need for a synchrotron radiation source each time a part is made and thereby significantly lowers the cost of the process. The dimensional control of this process is quite good and the tool insert can be used many times before it is worn out. [26]

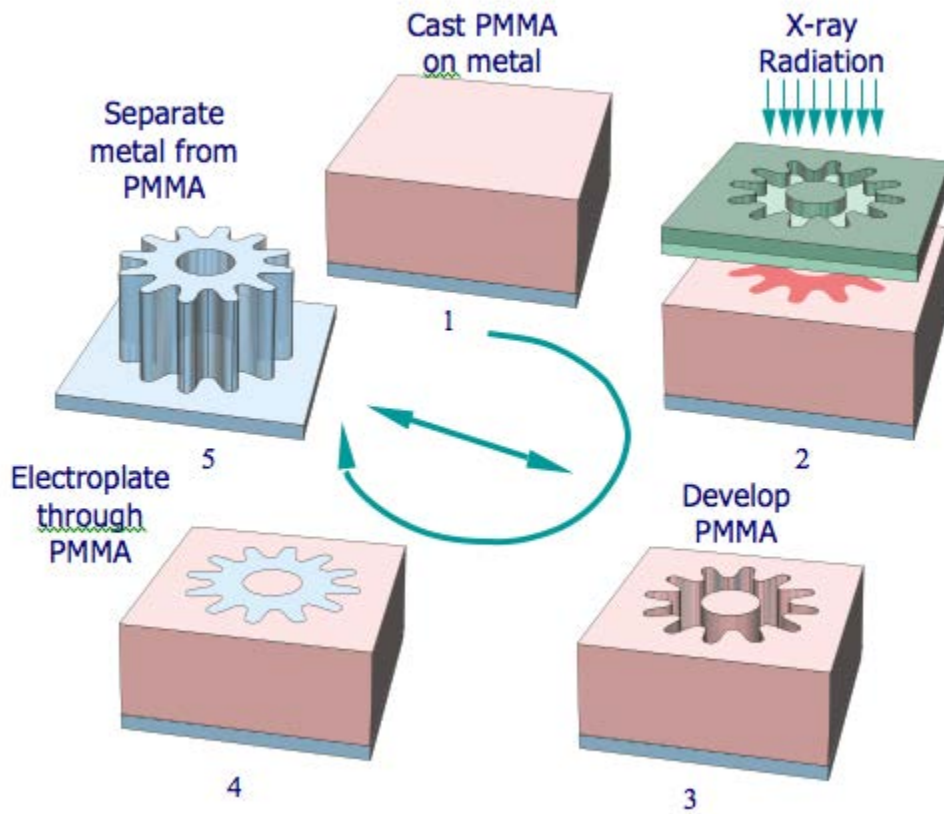


Figure 1.9.7(A): An illustration of the steps involved in the LIGA process to fabricate high aspect ratio MEMS devices.

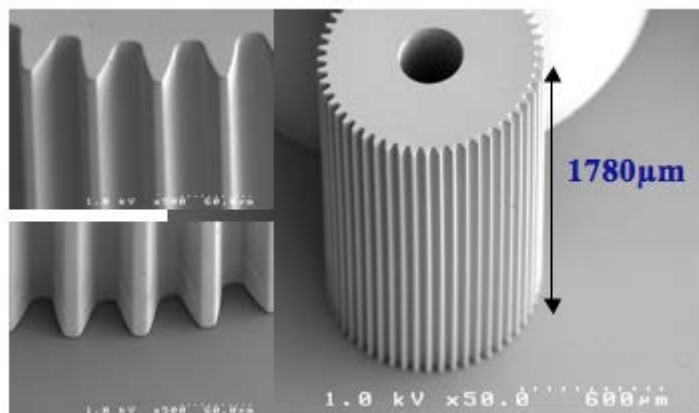


Figure 1.9.7(B): A tall, high aspect ratio gear made using LIGA technology.

## 2). Hot Embossing

A process to replicate deep high-aspect ratio structures in polymer materials is to fabricate the metal tool insert using LIGA or a comparable technology and then to emboss the tool insert pattern into a polymer substrate, which is then used as the part. Figure 13 is a diagram illustrating the hot embossing process. A mold insert is made using an appropriate fabrication method (shown in black cross-hatched pattern) having the inverse pattern made into it. The mold insert is placed into a hot embossing system (see Figure 14 for a photo of a hot embosser) that includes a chamber in which a vacuum can be drawn. The substrate and polymer are heated to above the glass transition temperature,  $T_g$ , of the polymer material and the mold insert is pressed into the polymer substrate. The vacuum is critical for the polymer to faithfully replicate the features in the mold insert since otherwise air would be trapped between the two surfaces resulting in distorted features. Subsequently, the substrates are cooled to below the glass transition temperature of the polymer material and force is applied to de-emboss the substrates. As shown in Figure 1.9.7 (C) hot embossing can successfully replicate complicated, deep and high-aspect ratio features. This process can make imprints into a polymer hundreds of microns deep with very good dimensional control. The advantage of this process is that the cost of the individual polymer parts can be very low compared to the same structures made using other technologies. Because of the overwhelming cost advantages combined with very good performance, this polymer molding process is very popular for producing microfluidic components for medical applications.

Heat plastic substrate and mold to insert to above plastic  $T_g$ , and pull vacuum on chamber. Apply forces to emboss plastic substrate. Cool plastic substrate and mold to insert to de-molding temperature and apply force to de-emboss.

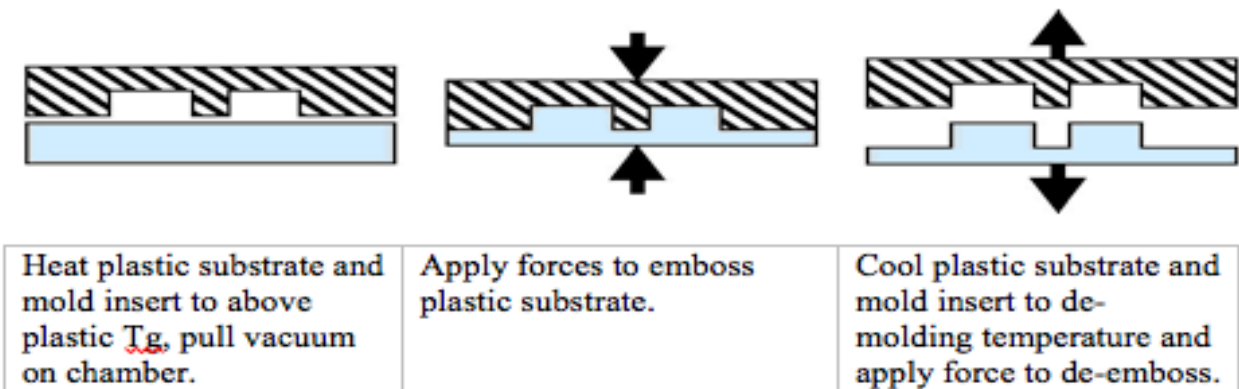


Figure 1.9.7 (C): Illustration of the hot embossing process to create micro devices. (Courtesy of the MNX at CNRI). [27]

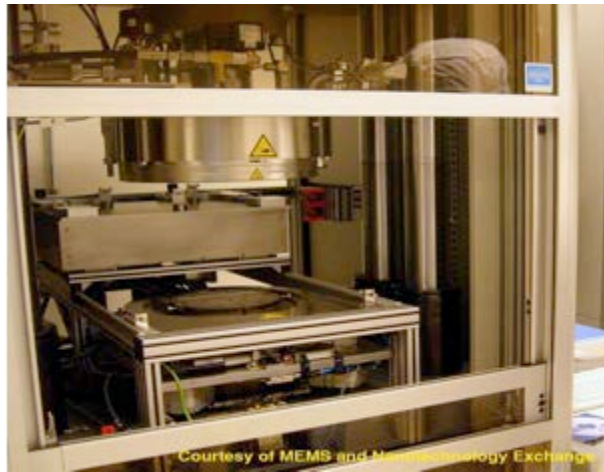


Figure 1.9.7(D): Photograph of a hot embossing platform during use.(Courtesy of the MNX at CNRI). [27]

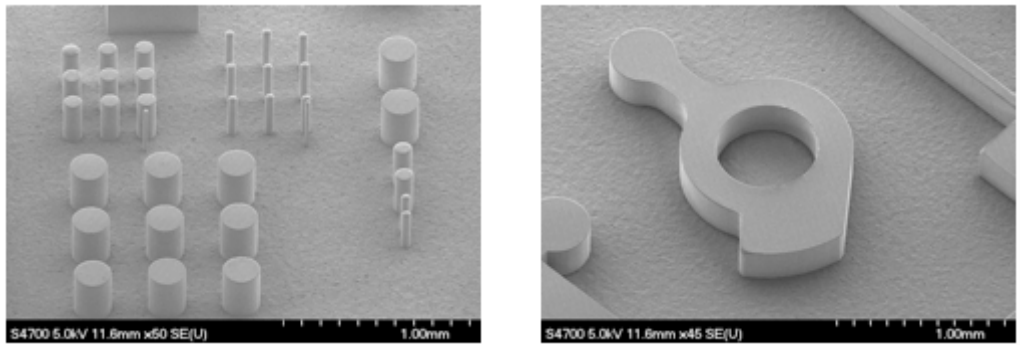


Figure 1.9.7(E): SEM of a variety of small test structures made in a plastic substrate using hot embossing technology at the MNX. The height of the plastic microstructures is nearly 300  $\mu\text{m}$  and the smallest features have a diameter of about 25  $\mu\text{m}$ . (Courtesy of the MNX at CNRI). [27]

### 3). Other Micromachining Technologies

In addition to bulk micromachining, surface micromachining, wafer bonding, and high aspect ratio micromachining technologies, there are a number of other techniques used to fabricate MEMS devices.

#### 4). XeF<sub>2</sub> Dry Phase Etching

Xenon Difluoride (XeF<sub>2</sub>) in a vapor state is an isotropic etchant for silicon. This etchant is highly selective with respect to other materials commonly used in microelectronics fabrication including: LPCVD silicon nitride, thermal SiO<sub>2</sub>, aluminum, titanium and others. Since this etchant is a completely dry release process, it does not suffer from the stiction problems of wet release

processes. This etchant is popular with micromachining of microstructures in pre-processed CMOS wafers where openings in the passivation layers on the surface of the substrate are made to expose the silicon for etching.

### 1.9.8 Disadvantages and advantages of the Polymer materials

A). Advantages: High biocompatibility, rapid prototyping, low fabrication cost and stability under a wide range of temperatures.

B). Disadvantages: polymers need more additional processing for the surface property control and manipulation. PDMS is inherently hydrophobic to water and with a low zeta potential value which hampers the ability of electrokinetic effects to achieve fluid flow. [Unfortunately, there are several disadvantages with the material properties of polymers as well. In general, polymers require additional processing steps for surface property control and manipulation. For example, poly(dimethylsiloxane) (PDMS) is inherently hydrophobic to water and with a low zeta potential value which hampers the ability of electrokinetic effects to achieve fluid flow. Even though the zeta potential can be increased through the use of surface treatments such as plasma, the resulting zeta potential is unstable, with the charge reverting close to its native value within 24 hours. Another problem with polymeric materials such as PDMS is its absorption and adsorption of certain fluorescent dyes such as Rhodamine B and certain proteins. [28]

### 1.9.9. Two dimensional numerical simulation of chaotic flow:

The CFD mixing simulations can be applied to realize the chaotic mixing in computer. Here is an example from the simulation of the VLM (Figure 4.4.1)

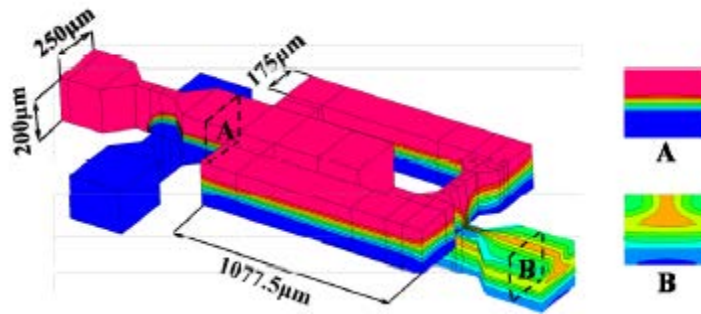


Figure 1.9.9 CFD simulation of Chaotic flow in a VLM at  $Re=0.64$

If we chose the CFD-ACE+, some physic characteristics of the micro-fluidics and the boundary conditions should be set, such as the diffusion coefficient, coefficient of viscosity, density and mole concentration. The main way we chose is to use the ansys to simulate the chaotic flow in the micro-mixes. Ansys can demonstrate: solid modeling, mapped meshing, defining an abbreviation on the Toolbar, restart of FLOTRAN solution, multiple solutions, vector display, line graphs, path operations, trace particle animation, multiple species, fluid mixing in microfluidic channels, fluid flow around obstacles in fluid channel.

To know the mixing efficiency, we will chose to measure the intensity of mixing micro-fluidic flow at every pixel. Besides, we can introduce some equations to quantify the mixing efficiency to analysis the mixing results. For example,

$$\sigma = \lim_{\substack{z \rightarrow \infty \\ |dX| \rightarrow 0}} \left[ \frac{1}{t} \ln \left( \frac{|dx|}{|dX|} \right) \right] \quad (1.9.9)$$

In this equation [6], chose the  $\sigma$  which is an index of the divergence of initial condition to make the mixing efficiency be quantitative.

## Chapter 2 Transport Phenomenon In Microfluidic Mixer

### 2.1 Transport phenomenon of microfluidics in the micro-mixers

#### 2.1.1 Fluid flow governing equations:

Fluid flow runs in the micro-channels, with the Reynolds number being a good symbol of flow regime. When the  $Re=2300$ , the flow is nearly a turbulent flow. So there is an equation which can calculate the Reynolds number:

$$R_e = \frac{\rho V D}{\mu} \quad (2.1.1 \text{ a})$$

Here the  $Re$  is the Reynolds number[29],  $\rho$  is the density,  $V$  is the velocity of the fluid,  $D$  is the characteristic length of the channel and  $\mu$  is the dynamic viscosity of the fluid. The Reynolds number ranges from 0.1 to 10, which represents the flow that is not turbulent flow. There is another important factor that is the Peclet number given into two forms:

$$P_e = \frac{V w}{D_a} \quad (2.1.1 \text{ b})$$

$$P_e = \frac{V_w}{\alpha_a} \quad (2.1.1 \text{ c})$$

Here [5] the  $Pe$  means the dimensionless Peclet number[30],  $V$  is the velocity of the fluid,  $D_a$  and  $\alpha_a$  are the mass diffusion coefficient and the thermal diffusivity of species "a", equation 5.1.1b is used to compare the effects of convection to mass diffusion whereas equation 5.1.1c .

#### 2.1.2 Electrophoresis in the transport of the microfluids:

When adding an external electric field, the fluids particles will move through the medium. There is a diffusion of the molecules between streams flowing side by side.

#### 2.1.3 Heat Transfer:

Heat transfer [3] in the micro scale is governed by conduction, convection, and radiation:



$$q_{cond} = -kA \frac{\partial T}{\partial x}$$

$$q_{conv} = hA(T_s - T_\infty)$$

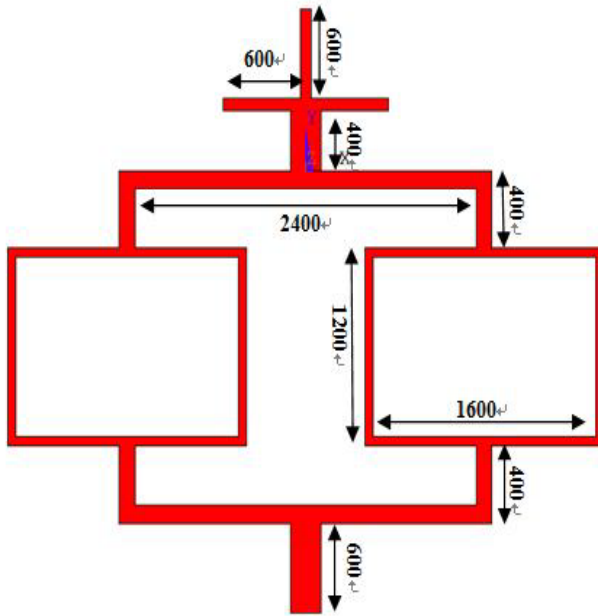
$$q_{rad} = \varepsilon \sigma A (T_s^4 - T_{sur}^4) \quad (2.1.3)$$

- ❖ q is the heat transfer;
- ❖ k is the thermal conductivity;
- ❖ Ts is the temperature;
- ❖ T $\infty$  is the air temperature;
- ❖ Tsur is the surrounding temperature;
- ❖ h is the convection coefficient;
- ❖  $\varepsilon$  is the emissivity;
- ❖  $\sigma$  is the Stefan-Boltzmann constant.

## Chapter 3 Passive Micro-mixer Design and Simulation

### 3.1 Introduction of Passive Micro-mixers and Active Micro-mixers

The proposed passive micro-mixer design is shown in Figure 1. With 3 inlets (1 vertical inlet and 2 horizontal inlets) and 1 outlet, it can effectively mix up to 3 different microfluid flows. Microfluid flows from 3 inlets are first mixed into one channel, then divided into 2 branches and then further divided into four sub-branches. After that, the flows from 4 sub-branches are mixed back into two branches, and finally rejoined back into one channel and flow out of the outlet. By introducing many rounds of turn-overs, turbulence is induced each time when microfluid flow changes its flow direction. The total length of the micro-mixer is about 20480  $\mu\text{m}$ . The channel width is also dynamically adjusted to adapt to different amounts of microfluid flow along the channel. For example, if multiple branches are joined together, the corresponding channel is enlarged to accommodate the increased microfluid flow. If a channel is divided into multiple branches, the corresponding branches are narrowed to adapt to the reduced microfluid flow.



Parameter	Dimension
Inlet Channels	80 μm
Secondary Vertical Channel	240 μm
Horizontal Channel after secondary channel	120 μm
Central/ Passing Rectangular Channels	60 μm
Horizontal Channel Near Outlet	120 μm
Outlet Channel	240 μm

Assume the microfluid flow in vertical inlet (labeled as fluid A) contains a protein like solution like and the concentration is set to 1. The microfluid flow in two horizontal inlets (labeled as fluid B) is the same and its concentrations is set to be 0 (i.e. pure water). Based on microfluid dynamics analysis, we estimate the mixing efficiency as well as the intensity of segregation and variation coefficient of the microfluid flows inside the mixer. In addition, Reynolds number is also a very important factor of fluid flow to measure the ratio between inertial and viscous forces in a particular flow. For Reynolds number below 2100, we get laminar flow in which the fluid molecules travel along well-ordered non-intersecting paths or layers. When Reynolds number is over 4000, we get turbulent flow that fluid molecules from adjacent layer become totally mixed. For microfluidics, generally we get laminar flow.

Reynolds Number is calculated as:

$$R_e = \rho V_{ref} L_{ref} / \mu$$

The equation of Mixing Efficiency:

$$\sigma = \left[ 1 - \sqrt{\frac{\sum_{i=1}^n (C_i - C_\infty)^2}{n}} / C_\infty \right] \times 100\%$$

where  $C_i$  is the mole percentage of the No.  $i$  dot in a certain area,  $n$  is the number of style points in a certain cross section,  $C_\infty$  is the ideal mole percentage,  $C_i$  is a number in range from 0 to 1. When  $C_i$  is 0.5, it indicates A fluid and B fluid are mixed completely.

The Intensity of Segregation and Variation Coefficient:

$$V_c = \sigma_o / x_v$$

$$I_s = \sigma_o^2 / \sigma_i^2$$

$\sigma_i$  and  $\sigma_o$  are the standard deviation of the mass fraction of species at the inlet and outlet of micromixer,  $x_v$  is the mass fraction of species at the inlet.

### 3.2 Results and Discussions

ANSYS FEM simulation is used to verify the function of the MEMS mixer. The velocities of both of species 1 and species 2 at inlets are set to be 1000 $\mu\text{m/s}$  (boundary condition). Density of species 1 and 2 are set as 1g/cm<sup>3</sup> and 1.5 g/cm<sup>3</sup> respectively. Our calculation shows that the Reynolds number of the microfluid flows is under 10, which belongs to laminar flow. The meshed ANSYS model of the MEMS mixer is shown in Fig. 3.2 B. The contour plot of the flow density is shown in Fig. 3.2B. From Fig. 3.2B, we can clearly see how both microfluid flows are mixed rapidly along the channels. The light blue (1.444) and yellow (1.000) colors represent microfluid species 1 and 2 respectively. Once both fluids are thoroughly mixed, its color becomes uniform dark blue (1.333).

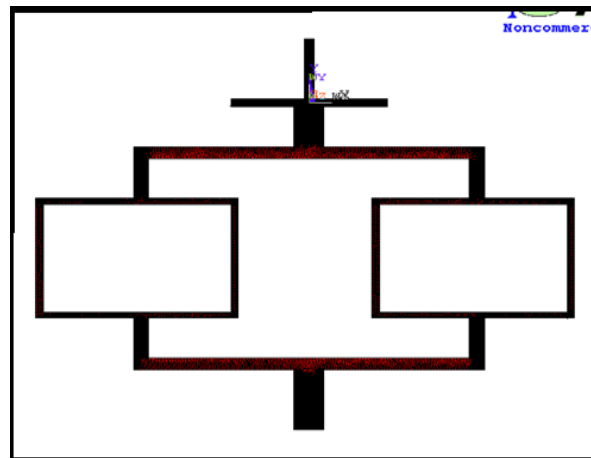


Fig.3. 2A Meshed ANSYS model of mixer

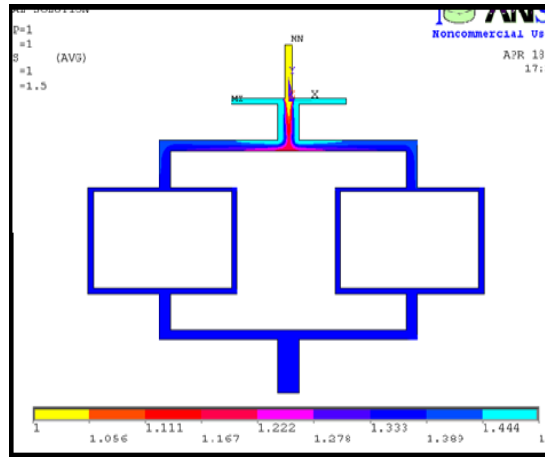


Fig. 3.2 B Contour plot of density distribution

The mixing can be verified not only from density contour plot, but also the density path plot along the cross section of the inlet and outlet. The ANSYS simulated density distribution plot along the cross section of the first top vertical channel section near the inlets is shown in Fig. 6. We observe that the microfluid is not well mixed yet at this time, because there are more species 1 in the middle, and more species 2 in both sides close to the channel sidewalls. After passing the MEMS mixer, the density path plot along cross section of outlet is shown in Fig. 4. It shows the microfluids (species 1 and 2) are now thoroughly mixed, and a uniform density distribution is achieved.

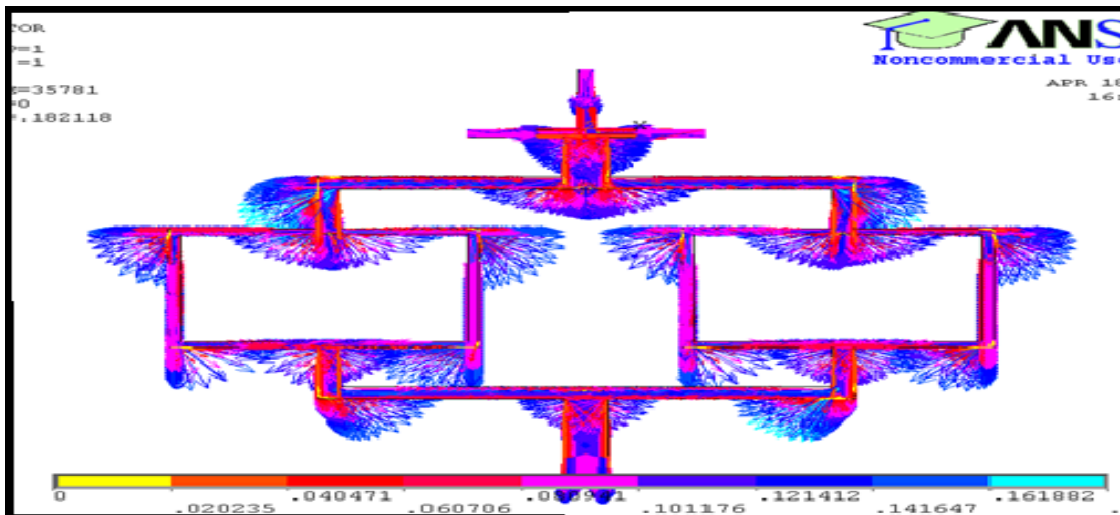


Figure 3.2 C Ansys Fluid Velocity Vector Plot

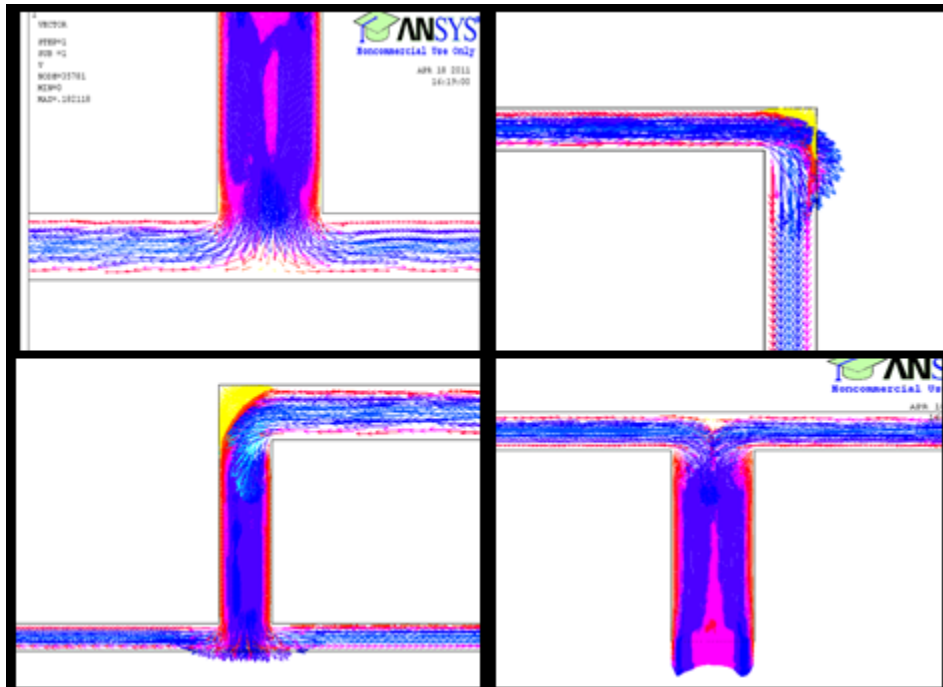


Figure 3.2 D Local View of Induced Turbulence

The mixing can be verified not only from density contour plot, but also the density path plot along the cross section of the inlet and outlet. The ANSYS simulated density distribution plot along the cross section of the first top vertical channel section near the inlets is shown in Fig. 6. We observe that the microfluid is not well mixed yet at this time, because there are more species 1 in the middle, and more species 2 in both sides close to the channel sidewalls. After passing the MEMS mixer, the density path plot along cross section of outlet is shown in Fig. 4. It shows the microfluids (species 1 and 2) are now thoroughly mixed, and a uniform density distribution is achieved.

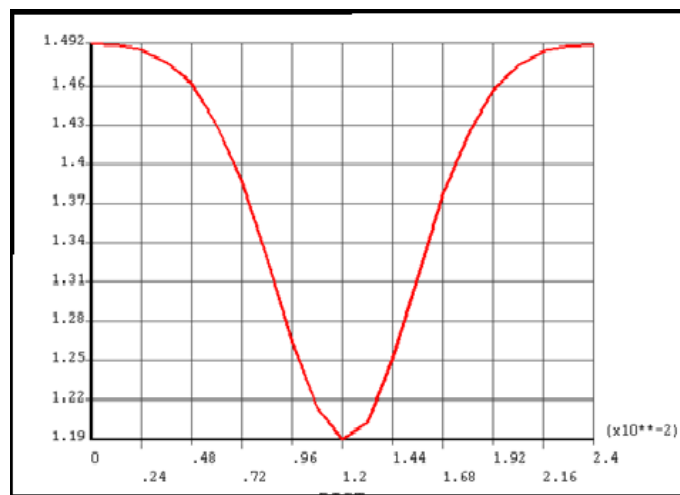


Figure 3.2 E Density Distributions near Inlet

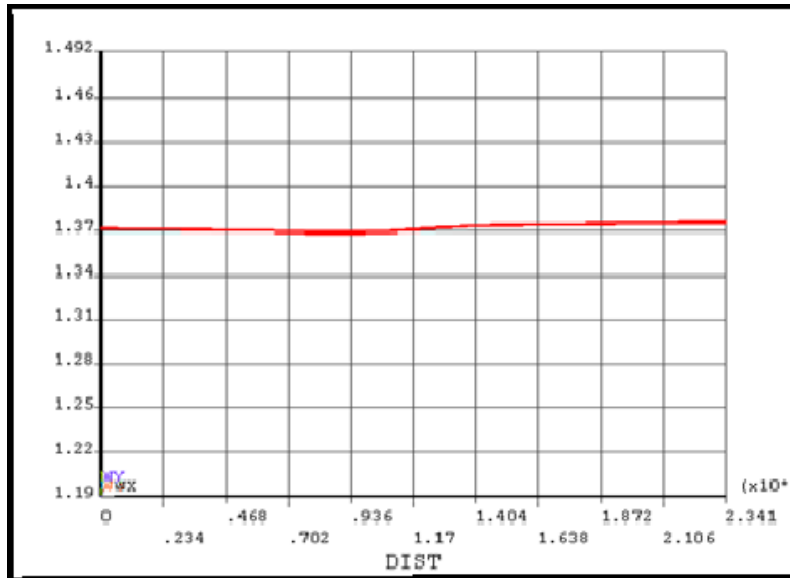


Figure 3.2 F Density Distribution at Outlet

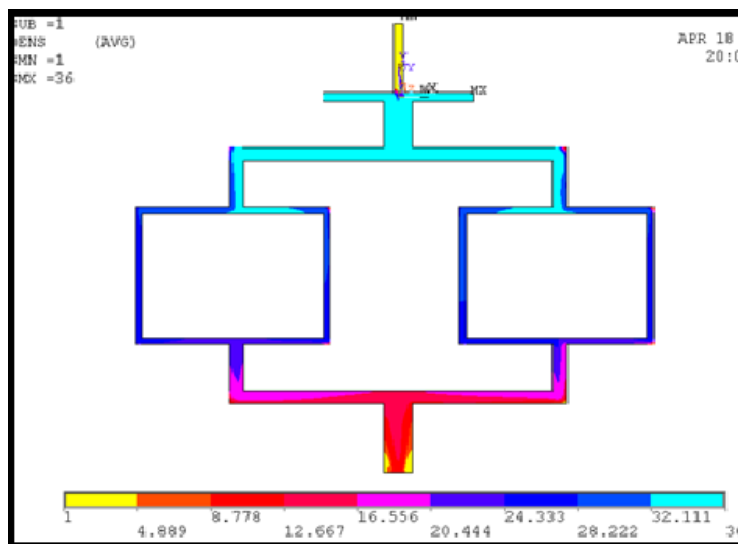


Fig. 3.2G Density plot ( $\rho_2=35\text{g/cm}^3$ )

Furthermore, we also simulated the case when the density of species 2 is changed from  $1\text{g/cm}^3$  to  $35\text{g/cm}^3$ , the result is shown in Fig. 3.2G. Compared with result in Fig. 3, we can see that as the initial density different among input microfluid becomes larger; it takes longer distance for both microfluids to thoroughly mix with each other. This indicates it's more challenging to mix two microfluids with larger difference in its properties.

## Chapter 4 Design and Analysis of an Electrostatic Active Microfluidic Mixer

### 4.1. Introduction of new micro-mixer with electromechanical power

Here is a new kind of active-passive combined micro-mixer, which has added some resonant plates in the micro-channels. Then two external electrodes will be installed paralleled with the resonant plates inside the micro-channels. There is an electric-potential difference formed between the resonant plates inside the micro-channel and the electrodes outside of the micro-channel. These actuated resonant plates can disturb the shear layer at the interface of the two fluids that generate turbulence in the micro-channel. After this kind of solving ways, the micro-fluids can be mixed more effectively to achieve the aim of increasing interface between two fluids in the area.

#### 4.1.1 .Electromechanical design

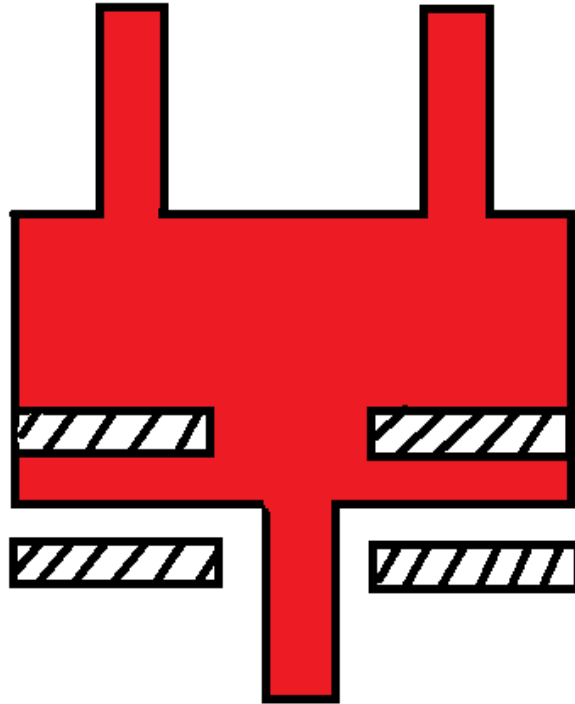
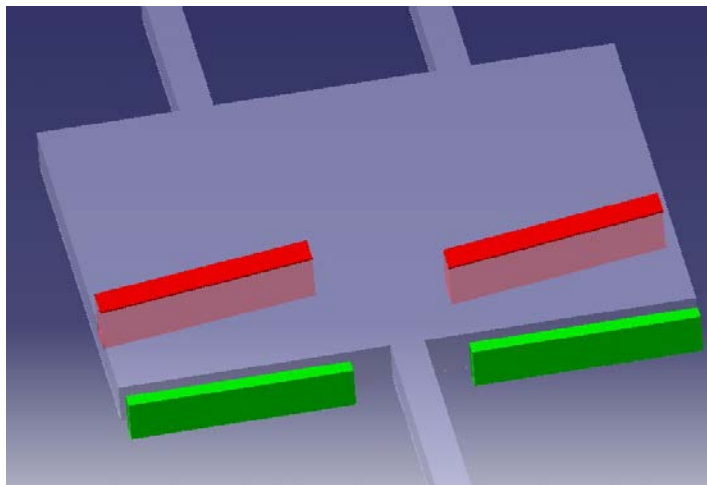
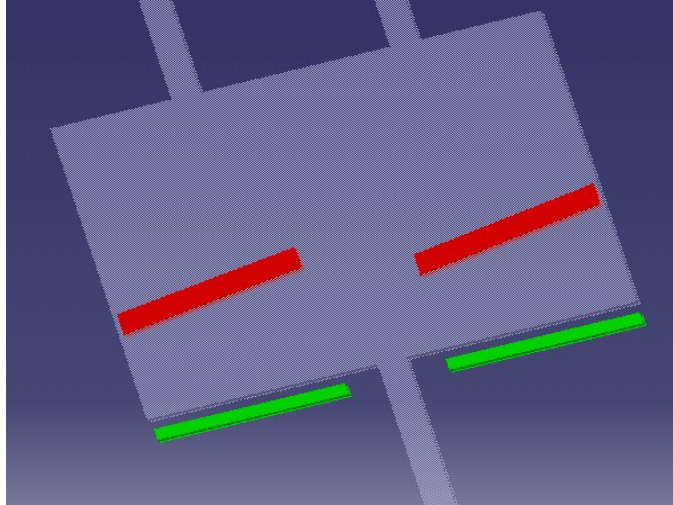


Figure 4.1.1(A) 2-dimension electrostatically activated resonant micro-mixer





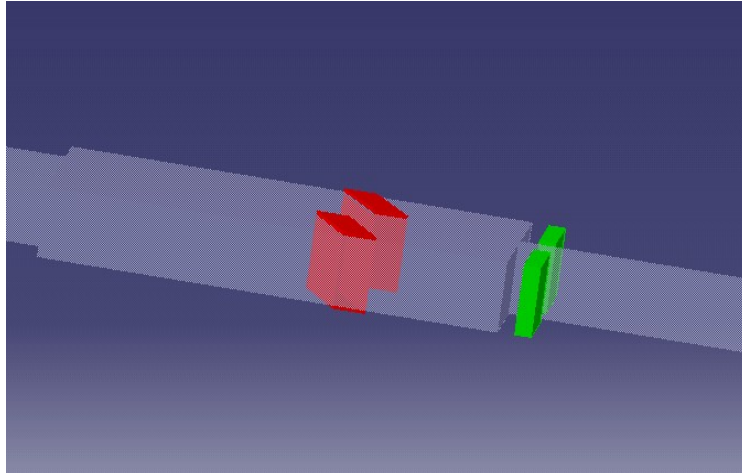


Figure 4.1.1(B). 3 views from different angles of the 3-dimension active micro-mixer

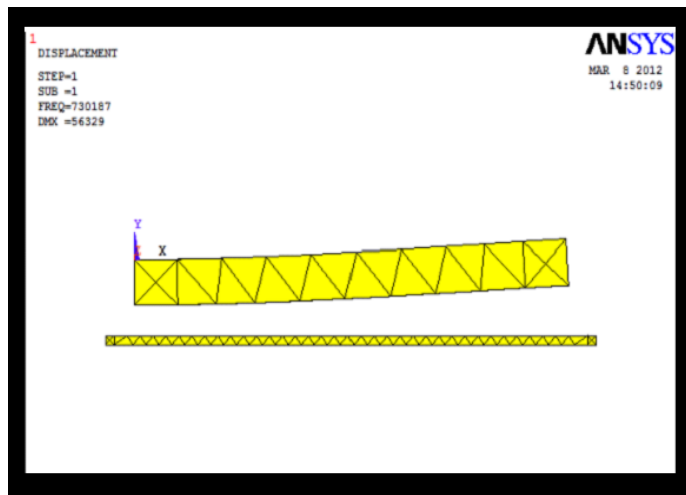
<b>Parameter</b>	<b>Dimension</b>
<b>Inlet Channels</b>	<b>80 <math>\mu\text{m}</math></b>
<b>Outlet Channel</b>	<b>160 <math>\mu\text{m}</math></b>
<b>Parameter</b>	<b>Length</b>
<b>Vertical Inlets</b>	<b>600 <math>\mu\text{m}</math></b>
<b>Width of Central/ Passing Rectangular Chamber</b>	<b>1200 <math>\mu\text{m}</math></b>
<b>Length of Central/ Passing Rectangular Chamber</b>	<b>1600 <math>\mu\text{m}</math></b>
<b>Vertical Outlet</b>	<b>600 <math>\mu\text{m}</math></b>

(For here, the amplitude of fluctuation of the two resonant plates will change from 0  $\mu\text{m}$  to 1  $\mu\text{m}$ , the thickness of the two resonant plates will vary from 1  $\mu\text{m}$ , 1.5  $\mu\text{m}$  to 2  $\mu\text{m}$ , and the length of the electrostatic power driven plates will be set to 300  $\mu\text{m}$ .)

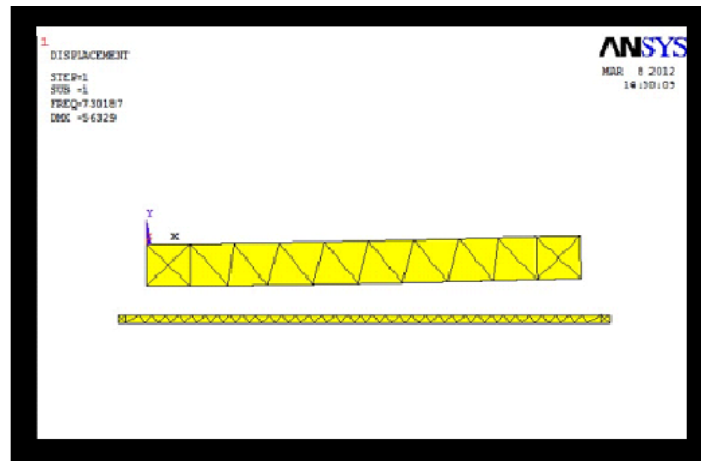
This kind of new electromechanical power driven micro-mixer has two vertical inlets and one vertical outlet. The main fluid chamber is a rectangular chamber which connects inlets and outlet. Besides, there are two resonant plates are inside the chamber and two electrodes outside of the chamber. As the voltage changes, those two resonant plates will fluctuate along the direction which is perpendicular to the horizontal wall of the chamber.

In these two inlets and one outlet micro-channel, two resonant plates will be set in the big micro-chamber and will flatten quickly in opposite directions under the applied voltage which is 200 volts.

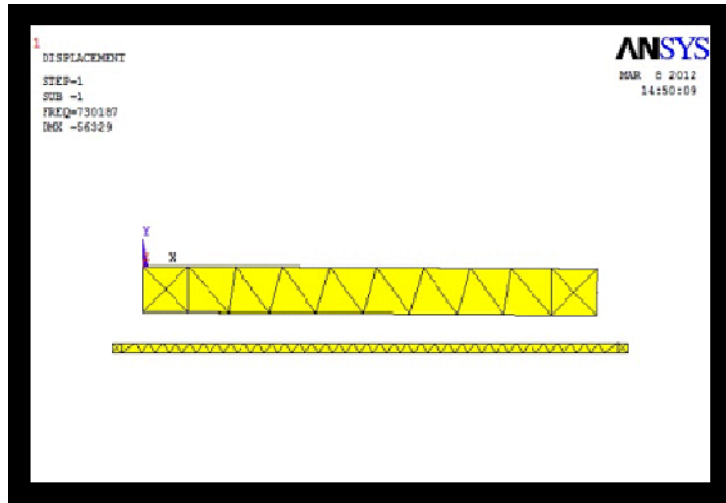
#### 4.1.2 Ansys simulation of electrostatic resonant plate



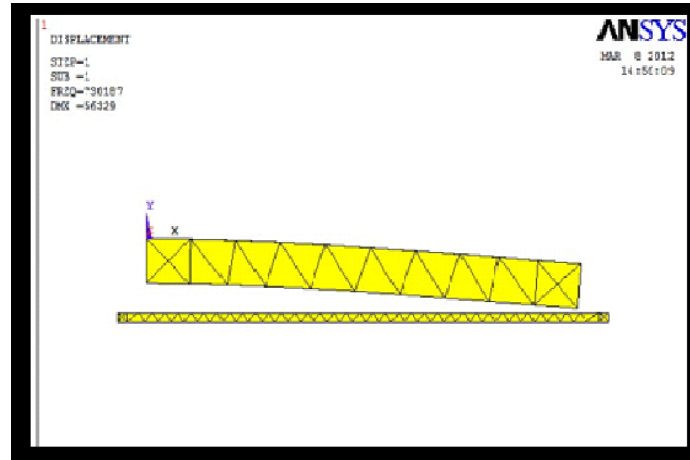
a



b



c



d

Figure 4.1.2 (1) Figure a,b,c,d are four stages which in the process of the fluctuation of the electrostatic resonant plate

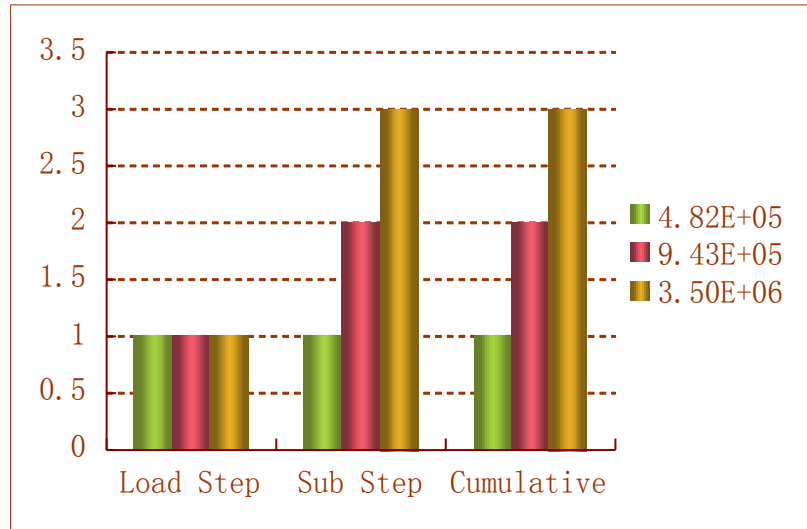


Figure 4.1.2 (2) This figure just shows three different frequencies

Here the actuation at natural frequency of cantilevered plate played a very important role to take advantage of the resonance of the plate for maximum actuation amplitude. There are many factors which will affect the amplitude of the resonant plates, including: electrostatic drive voltage, the thickness of the resonant plate, the distance between the resonant plate and the electrode, the length of the resonant plate, electrostatic force between the plate and the electrode, the width of the plate, the elasticity of the resonant plate.

$$q = \frac{\epsilon_0 \epsilon_r \omega}{2} \left( \frac{V}{g - \chi^2 d} \right)^2$$

4.1.2 a

- ❖  $q$  is the electrostatic force comes from the electrode outside , between the plate and the electrode (N/m) ;
- ❖  $g$  is the gap between the plate and the electrode;
- ❖  $\omega$  is the width of the plate;
- ❖  $V$  is the driving voltage;

In equation 4.1.2 a [32],  $\bar{x} = x/L$ , is the nondimensional distance along the plate,

$$d = \frac{1}{6EI} \int_0^L x^2 (3L - x) q(x) dx \quad 4.1.2b$$

- ❖ d is the tip deflection under partial loading;
- ❖ E is the module of elasticity;
- ❖ I is the moment of inertia ( $I = \omega h^3$ );
- ❖ L is the length of the load distribution along a plate;

In the equation 4.1.2b [32], d is the tip deflection under partial loading; this equation comes from the conventional beam theory [8].

$$d = \frac{\varepsilon_0 \varepsilon_r \omega V^2}{12EI} \int_0^L (3Lx^2 - x^3) \left( \frac{1}{g - \frac{x^2}{d}} \right)^2 \quad 4.1.2c$$

In the equation 4.1.2c [32], we just express the q(x) with equation 4.1.2a instead of q, and then to get the equation 4.1.2c, finally solve the equation 4.1.2c, we can get the following equation [32]:

$$V = \sqrt{\frac{8\Delta^2 EI g^3}{\varepsilon_0 \varepsilon_r \omega L^4} \left( \frac{2}{3(1-\Delta)} - \frac{\tanh^{-1} \sqrt{\Delta}}{\sqrt{\Delta}} - \frac{\ln(1-\Delta)}{3\Delta} \right)^{-1}} \quad 4.1.2 d$$

Here the  $\Delta = d/g$ .

### 4.1.3 Matlab for driving voltage versus the normalized deflection for different plate thickness and resonant frequency versus the length of the plate

Now using the equation 4.1.2d, we let the  $L = 300\mu\text{m}$ ,  $g = 50 \mu\text{m}$ ,  $\omega = 600 \mu\text{m}$ ,  $E = 169 \text{ GPa}$ ,  $\varepsilon_0 = 8.85 \times 10^{-12} \text{ C}^2 / \text{N.m}^2$ ,  $C1 = 1 \text{ C}^2 / \text{N.m}^2$  for the air ( $\omega$  is the width of the plate,  $g$  is gap

between the plate and the electrode, L is the nondimensional distance along the plate, and q is in N/m.) following is the matlab commands and figure.

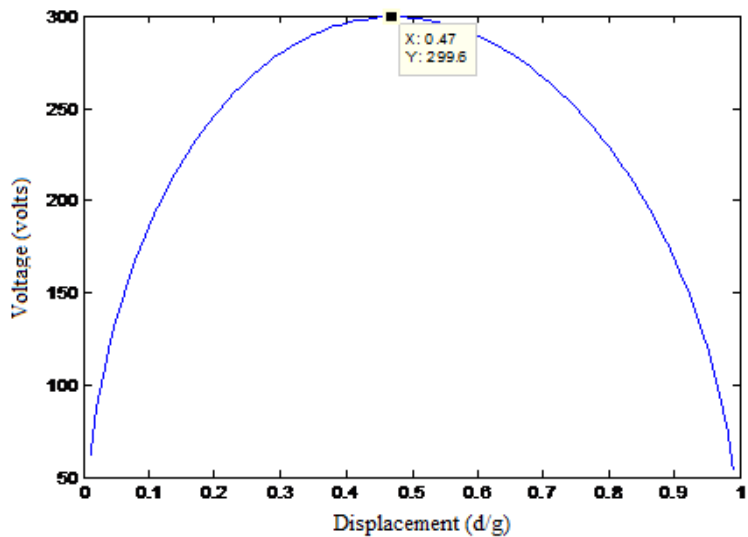
There are three figures which show the relationship between voltage and the displacement in different thickness of the resonant plate (h).

**Figure A**

$$y = \sqrt{196461 \times x^2 \times \left( \frac{2}{3 \times (1-x)} + \frac{\tanh^{-1} \sqrt{x}}{\sqrt{x}} - \frac{\ln(1-x)}{3x} \right)^{-1}}$$

4.1.2 e

[Here x is the displacement of the resonant plate which vibrates between middle of the channel and the wall of the channel; y is the voltage of the electrode which is added to the plate and locates at the outside of the micro-mixer. When the thickness of the resonant plate h= 1



μm]

Figure 4.1.3 A Relationship between voltage and displacement of resonant plate (h=1μm, Matlab)

Description: Here when the displacement is 0.47(peak displacement), the micro-mixer needs a voltage of 299.6 volts to drive. Before the displacement reach 0.47, increasing the voltage can make the resonant plate vibrating in bigger amplitude. Once the displacement comes to the peak

displacement, that is 0.47, the resonant plate will come closer and closer to the wall of the mixer with the increasing voltage.

**Figure B**

$$y = \sqrt{663057 \times x^2 \left( \frac{2}{3 \times (1-x)} + \frac{\tanh^{-1} \sqrt{x}}{\sqrt{x}} - \frac{\ln(1-x)}{3x} \right)^{-1}}$$

4.1.2 f

[Here the y and the x are represented the same things, and the h= 1.5 μm]

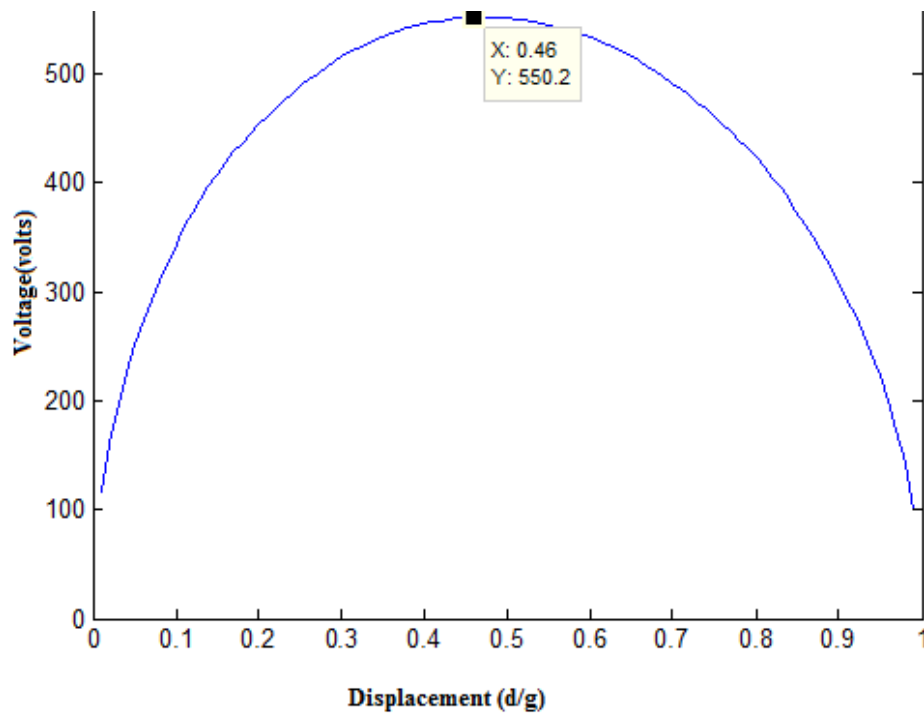


Figure B Relationship between Voltage and Displacement of Resonant Plate (h=1.5μm, Matlab)

In figure B, it shows that the maximum displacement is 0.46, when the driven voltage is 550.2 volts. The same principle with the Figure 4.1.3A, just here the peak value of the displacement is 0.46.

**Figure C**

$$y = \sqrt{1571691 \times x^2 \left( \frac{2}{3 \times (1-x)} + \frac{\tanh^{-1} \sqrt{x}}{\sqrt{x}} - \frac{\ln(1-x)}{3x} \right)^{-1}}$$

4.1.2 g

Here the thickness of the resonant plate is 2 μm.

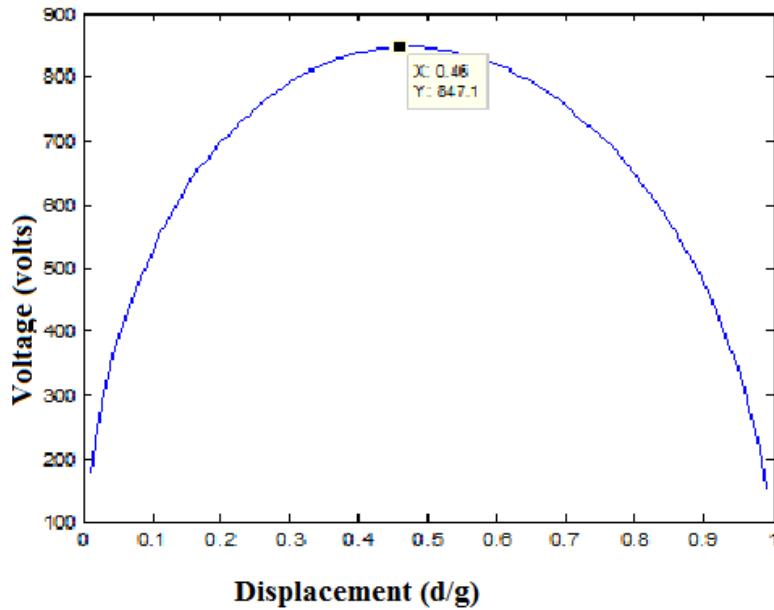


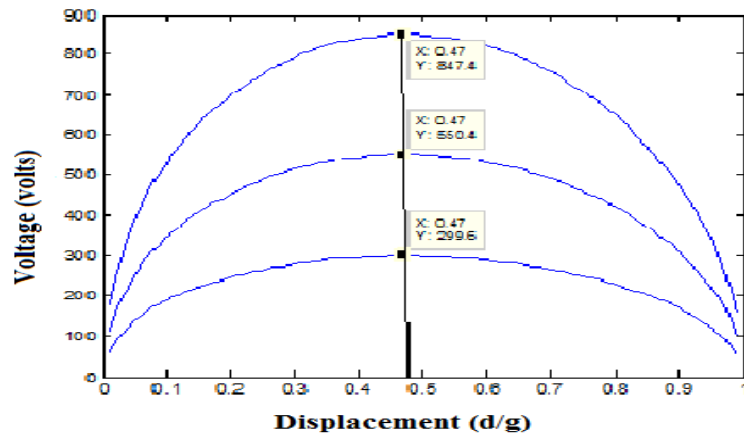
Figure C. Relationship between Voltage and Displacement of Resonant Plate (h=2μm, Matlab)

In figure C, it is reported that the biggest displacement is 0.46, when the driven voltage is 844.1 volts.

### Figure D



Comparison of the change of the tip deflection with given different electrostatic driving voltage



at various plate thickness.

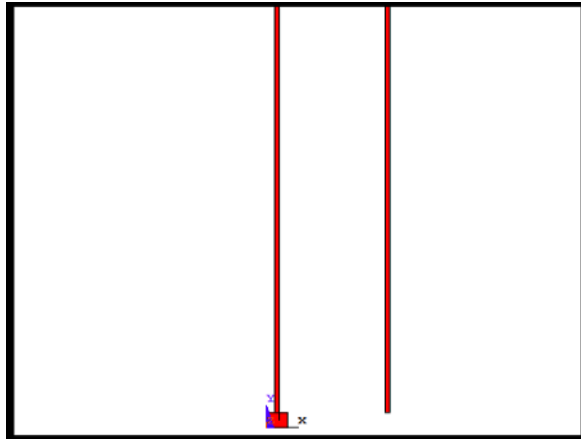
Figure D Comparison in three different thickness Matlab ( $h=1\mu\text{m}, 1.5\mu\text{m}, 2\mu\text{m}$ )

From the figure D, we can see the three acmes which show the snap-through voltage: 299.6 volts ( $h=1\mu\text{m}$ ), 550.4 volts ( $h=1.5\mu\text{m}$ ), 844.4 volts ( $h=2\mu\text{m}$ ). With the increase of the thickness of the resonant plate, the snap-through voltages also increase. After the snap-through voltages, higher voltage cannot make the actuated plate flatten more than the tip deflection under the snap-through voltage. Besides, before the snap-through voltage, if increasing the voltage, the displacement would fluctuate closer and closer to the channel wall.

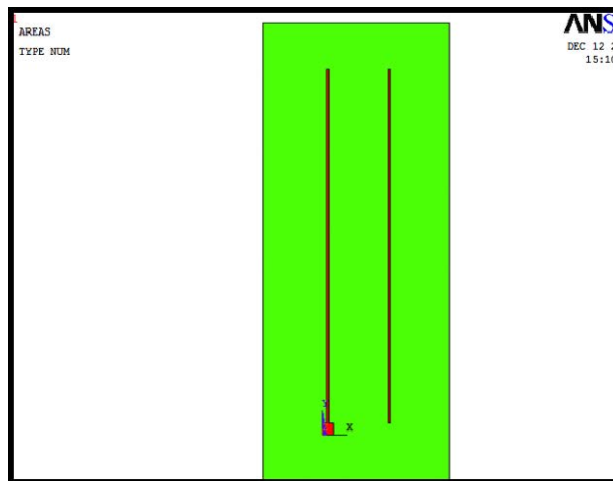
Matlab is used to draw the picture about the relationship between voltage and displacement when the electrostatic power driven resonant plate is vibrating in three different thicknesses ( $1\mu\text{m}$ ,  $1.5\mu\text{m}$ ,  $2\mu\text{m}$  Figure 4.1.2). In the first thickness ( $1\mu\text{m}$ ), the maximum displacement is  $0.47d/g$ , and the peak voltage is 299.6volts; in the second thickness ( $1.5\mu\text{m}$ ), the snap-through voltage comes to be 550.2 volts, and corresponding displacement becomes  $0.46d/g$ ; in the third thickness ( $2\mu\text{m}$ ), the highest voltage and displacement are 844.1 volts and  $0.46d/g$ . From these three teams data, we can see that the snap-through voltages increasing following the rise of the thickness, which means, when adding the thickness of the resonant plate, the plate needs a higher voltage to drive to reach the biggest displacement. However, if applying higher voltage than the snap-through voltage, the resonant plate cannot flatten more and get closer and closer to the wall of the chamber. At last, as above four figures show, the displacement would be  $0d/g$ , that is to say the plate and the wall of the chamber stick to each other.

#### 4.1.4 Simulation of the new micro-mixer in Ansys

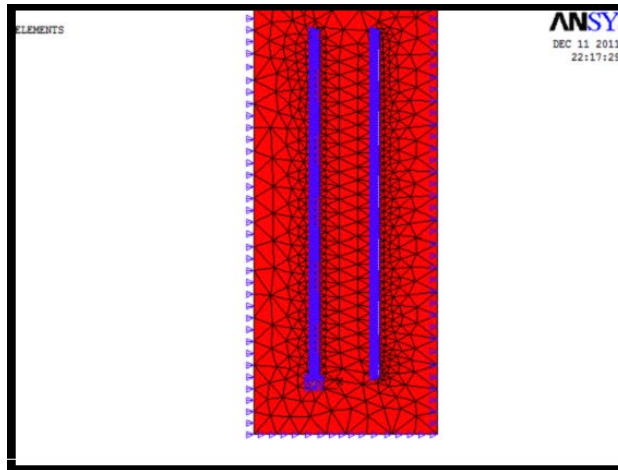
Below are three figures which are describing the simulation of the new micro-mixer in ansys. Especially this ansys simulation we can get the exact value for the maximum displacement of electrostatically activated micro-mixer plate flattening under the external electrodes (200volts).



(a)



(b)



(c)

The above three ansys figures are showing the relative displacement between the resonant plate and electrode plate.

```

***** ROUTINE COMPLETED ***** CP =          9.859

***** ANSYS ANALYSIS DEFINITION <PREP7> *****
ENTER /SHOW,DEVICE-NAME TO ENABLE GRAPHIC DISPLAY
ENTER FINISH           TO LEAVE PREP7
PRINT/QUI KEY SET TO /GPR (USE /NOPR TO SUPPRESS)
-----
RECURSIVE SOLUTION SUMMARY
-----
loop No.  Max.Displacement  Struct.Convergence  Elec.Energy  Elec.Convergence
  1.      0.5310E+00         0.2655E-02         0.2499E+01   0.1250E-01
  2.      0.5406E+00         0.1806E-01         0.2503E+01   0.1736E-02

LISTING OF THE DATA ON FILE _essolu.out
-----
ESSOLU SOLUTION SUMMARY
-----
Title of the electrostatics physics file - ELECTROS .
Title of the structural physics file - STRUCTUR .
Model dimensionality = 2 .
Morphing option = 0 .
Component of non-structural morphing entities= AIR .
Component of entities excluded from morphing procedure: .
Convergence tolerance for electrostatic solution: 5.E-03 .
Convergence tolerance for structural solution: 5.E-03 .
Maximum loop number allowed = 50 .

Loop No.  Max.Displacement  Struct.Convergence  Elec.Energy  Elec.Convergence
  1.      0.5310E+00         0.2655E-02         0.2499E+01   0.1250E-01
  2.      0.5406E+00         0.1806E-01         0.2503E+01   0.1736E-02
  3.      0.5407E+00         0.3244E-03         0.2503E+01   0.3023E-04

```

(d)

Figure 4.1.3 Ansys for the plate which applied to a electrode plate (a. b. c. are three ansys simulation results and d is the results of the displacement of the resonant plate which is under the electrostatic force)

**Here in this table, the last max displacement: 0.5407E+00 are the best value for testing the resonant plate.**

Ansys simulation here is to verify and test how the resonant plate flattens and the vibration amplitude of the plate. Firstly, the ansys for testing the vibration conditions of the electrostatic resonant plate is shown in Figure 4.1.2, there are three conditions of the vibration of the 3-dimension resonant plate. In this ansys simulation, the length of the resonant plate is set to be 300 $\mu\text{m}$ , thickness comes to be 2 $\mu\text{m}$ , and width is 50 $\mu\text{m}$ . When giving different frequencies, the plate would flatten in different amplitudes. Then, there is another ansys simulation which shows the vibration of the resonant plate under an external applied electrode plate, and the two plates are paralleled with each other. Here in the Chapter 7, there is a big table which includes the main results, maximum displacement of the electrostatic activated plate we got is 0.5407E+00, the optimal value of those four results. Also, in this ansys, I just set the length of the plate to be 300 $\mu\text{m}$ , the thickness of the plate 2 $\mu\text{m}$  and the voltage 200 volts.

We can see that there is a comparison between these two ansys simulations, the first one is that the resonant plate vibrates in three given different frequencies, the second one is that the resonant plate flattens under an external electrode plate and we can get the exact displacement when given a snap-through voltage.

## **Chapter 5 Conclusions and Future Work**

Here in this report, a new electrostatic driven micro-pump mixer is introduced and integrated with the resonant plate in the channel of micro-mixer to advance the mixing efficiency, however, the effective micro-pump mixer in this report is very simple and just two inlets and one outlet. This kind of micro pump-mixer can be used in mixing both liquid and gas. In this report, I just set up the electrostatic activated resonant plates (there are two plate paralleled with the bottom of the chamber) near the bottom of the main rectangular micro-fluid chamber to enhance the mixing of two kinds of micro-fluids when the fluids are running out the mixer, then there would be a vortex around the tip of two plates. After adding an external electrode to apply on the resonant plate, we can get an optimum maximum displacement:  $0.5407E+00$ , that shows the higher effectiveness with an external power than without additional power.

In the future, I will further do some research about how to make the micro-fluidic mixer mixing more efficient than this one, that means to change some external power including the voltages of the external electrode, location of the electrode; except these, I will try many other shapes of micro-fluidic mixers or to change the conditions for setting the mixing plates which in the channels, like the location and the quantity of the plates. However, there are many ways to make the micro-fluidic mixer better; they should not be too expensive in application.

## References:

- [1]. Yong Li, Xingxin Wang, Ruijing Wang . Effects of the Mixing of Micro-fluidics and Micro-mixer Journal of Library Science in China TK 124, PP 1 , 2008 (7)
- [2]. Y. Wang, Q.Lin, T. Mukherjee Applications of Behavioral Modeling and Simulation on Lab-on-A-Chip: Micro-mixer and Separation System IEEE 2004 PP 8
- [3]. Hongyu Yu, Jae Wan Kwon, Eun Sok Kim Microfluidic Mixer and Transporter Based on PZT Self-Focusing Acoustic Transducers Journal of MEMS Vol. 15, No. 4, August 2006
- [4]. Alireza Bahadorimehr, Azrul Azlan Hamzah, Burhanuddin Yeop Majlis Vol 3, Suppl 1, 2011 Fabrication of An Integrated Microfluidic Perfusion System for Mixing Different Solutions International Journal of Pharmacy and Pharmaceutical Sciences ISSN-0975-1491 PP 1
- [5]. Hinsmann P et al 2001 Design, Simulation and Application of A new Micromixing Device for Time Resolved Infrared Spectroscopy of Chemical Reactions in Solutions Lab on a Chip 1 16–21
- [6]. Nam-Trung Nguyen and Zhigang Wu 8 December 2004 Micromixers—a Review Journal of Micromechanics And Microengineering pp 1-16
- [7]. Lim D S W et al 2003 Dynamic Formation of Ring-shaped Patterns of Colloidalparticles in Microfluidic Systems Appl. Phys. Lett. 83 1145–7
- [8]. Branebjerg J et al 1996 Fast Mixing by Lamination Proc. MEMS'96, 9th IEEE Int. Workshop Micro Electromechanical System (San Diego, CA) pp 441–6
- [9]. E Miyake R et al 1993 Micro mixer with fast diffusion Proc. MEMS'93, 6<sup>th</sup> IEEE Int. Workshop Microelectromechanical System (San Diego, CA) pp 248–53
- [10]. Voldman J, Gray M L and Schmidt M A 2000 An integrated liquid mixer/valve J. Microelectromech. Syst. 9 295–302
- [11]. Wang H et al 2002 Optimizing layout of obstacles forenhanced mixing in microchannels Smart Mater. Struct. 11 662–7
- [12]. Wong S H et al 2003 Investigation of mixing in a cross-shaped micromixer with static mixing elements for reaction kinetics studies Sensors Actuators B 95 414–24
- [13]. Wang H et al 2003 Numerical investigation of mixing in microchannels with patterned grooves J. Micromech. Microeng. 13 801–8

- [14]. Lin Y et al 2003 Ultrafast microfluidic mixer and freeze–quenching device *Anal. Chem.* 75 5381–6
- [15]. Mengeaud V, Josserand J and Girault H H 2002 Mixing processes in a zigzag microchannel: finite element simulation and optical study *Anal. Chem.* 74 4279–86
- [16]. Ryo Miyake, Theo S.J. Lammerink, Miko Elwenspoek, Jan H.J. Fluitman 1993 Micro mixer with fast diffusion *Proc.MEMS'93, 6th IEEE Int. Workshop Micro Electromechanical System (San Diego, CA)* pp 248–53
- [17]. Deval J, Tabeling P and Ho C M 2002 A Dielectrophoretic Chaotic Mixer *Proc. MEMS'02, 15th IEEE Int. Workshop Micro Electromechanical System (Las Vegas, Nevada)*pp 36–9
- [18]. Jacobson S C, McKnight T E and Ramsey J M 1999 Microfluidic devices for electrokinematically driven parallel and serial mixing *Anal. Chem.* 71 4455–9
- [19]. Bau H H, Zhong J and Yi M 2001 A minute magneto hydrodynamic (MHD) mixer *Sensors Actuators B* 79 207–15
- [20]. Razim Farid Samy, 2007, *Soft Lithography for Applications in Microfluidic Thermometry , Isoelectric Focusing, and Micromixers, IEEE, PP 1-176*
- [21]. Hinsmann P et al 2001 Design, simulation and application of a new micromixing device for time resolved infrared spectroscopy of chemical reactions in solutions *Lab on a Chip* 1 16–21
- [22]. Veenstra T T 1999 Characterization method for a new diffusion mixer applicable in micro flow injection analysis systems *J. Micromech. Microeng.* 9 199–202
- [23]. El Moctar A O, Aubry N and Batton J 2003 Electro–hydrodynamic micro fluidic mixer *Lab on a Chip* 3 273–80
- [24]. Walker, Perrin; William H. Tarn (1991). *CRC Handbook of Metal Etchants.* pp. 287–291.
- [25]. Degarmo, E. Paul; Black, J T.; Kohser, Ronald A. (2003), *Materials and Processes in Manufacturing (9th ed.)*, Wiley, P690.
- [26]. Madou, M. (2003). *Fundamentals of Microfabrication.* CRC.
- [27]. Throne JL 1996 *Technology of Thermoforming.*
- [28]. Rubinstein, Michael; Colby, Ralph H. (2003). *Polymer physics.* Oxford; New York: Oxford University Press. p.6.

- [29]. Batchelor, G. K. (1967). *An Introduction to Fluid Dynamics*. Cambridge University Press. pp. 211–215
- [30]. Patankar, Suhas V. (1980). *Numerical Heat Transfer and Fluid Flow*. New York: McGraw-Hill. p. 102
- [31]. Laser D J and Santiago J G 2004 A review of micropumps *J. Micromech. Microeng.* 11 R35–64
- [32]. Chia-Wen Tsao and Kamaran Mohseni, An Electrostatically Activated Resonant Micropump-mixer, Aerospace Sciences Meeting and Exhibit, CO 80309-429, 10-13, Jan 2005 PP 1-12